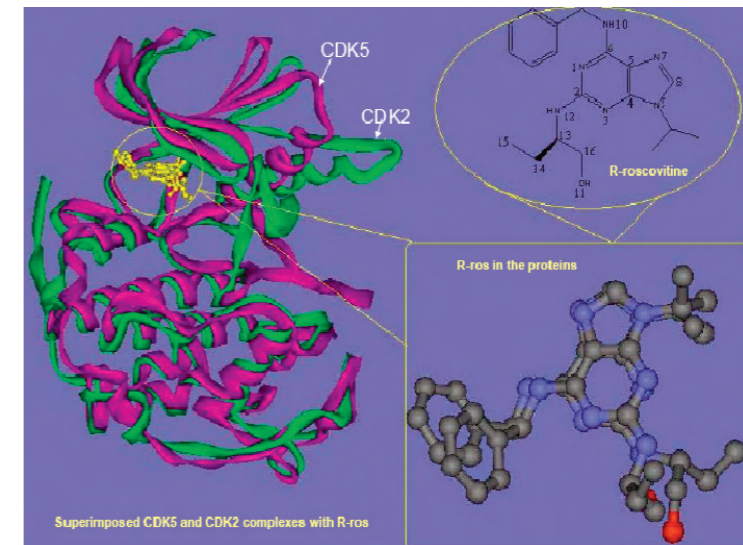


Thesis for doctoral degree (Ph.D.)
2009

PHARMACOLOGICAL AND ANALYTICAL STUDIES OF THE CYCLIN DEPENDENT KINASE INHIBITORS



Hatem Sallam

Thesis for doctoral degree (Ph.D.) 2009

PHARMACOLOGICAL AND ANALYTICAL STUDIES OF THE CYCLIN DEPENDENT KINASE INHIBITORS Hatem Sallam



Karolinska
Institutet



Karolinska
Institutet

From Department of Laboratory Medicine
Clinical Research Center – Experimental Cancer Medicine
Karolinska Institutet, Stockholm, Sweden

PHARMACOLOGICAL AND ANALYTICAL
STUDIES OF THE CYCLIN DEPENDENT
KINASE INHIBITORS

Hatem H. A. Sallam



**Karolinska
Institutet**

Stockholm 2009

All previously published papers were reproduced with permission from the publisher.

Published by Karolinska Institutet.

© Hatem H. A. Sallam, 2009

ISBN 978-91-7409-706-1

Printed by



www.reproprint.se

Gårdsvägen 4, 169 70 Solna

ABSTRACT

Cyclin-dependent kinases (Cdks) play a key role in the regulation of cell cycle progression and RNA transcription. Deregulation of Cdks has been associated with several malignancies, neurodegenerative disorders, viral and protozoal infections, glomerulonephritis and inflammatory diseases. (R)-roscovitine (Rosco) is a synthetic tri-substituted purine that inhibits selectively Cdk1, 2, 5, 7 and 9. Rosco has shown promising cytotoxicity in cell lines and tumor xenografts. Rosco so far has only demonstrated modest antitumor activity in phase-II clinical trials, which is attributed mainly to the short elimination half-life and thus suboptimal exposure.

Within the frame of the present thesis we aimed to investigate several aspects of the pharmacokinetics (PK) and pharmacodynamics (PD) of Rosco and two recently discovered analogues namely N-&-N1 and CR8. Our studies included bioanalysis, hematotoxicity, chrono-biodistribution, age dependent kinetics, PK and effect on Cdks.

In vitro and *in vivo* studies of Rosco hematotoxicity were performed in Balb/c mice. Bone marrow cells were incubated with Rosco in semisolid methylcellulose media and assessed for their clonogenic capacity. Rosco inhibited the colony formation in cell type-, concentration- and exposure time-dependent manner. CFU-GEMM were most sensitive, followed by BFU-E and the least sensitive progenitors were CFU-GM. *In vivo* studies showed low distribution of the drug to the bone marrow (AUC_{BM}/AUC_{plasma} 1.5%) and only transient inhibition of BFU-E formation was observed. These finding may explain the absence of myelosuppression *in vivo*.

Age-dependent PK of Rosco was investigated in 14days rat pups and adult rats. Higher plasma and brain (22- and 100- fold, respectively) exposure was found in rat pups compared to adult rats. The elimination half-life in young rats was 7 hr compared to 30 min in adult rats. Brain exposure (AUC_{brain}/AUC_{plasma}) was 100% in rat pups compared to 20% found in adult rats. Moreover, transient Cdk5 inhibition and Erk1/2 activation was detected in brain of rat pups. The high brain exposure may indicate Rosco as a potential candidate for the treatment of brain tumors in children.

The chronopharmacokinetics of Rosco was investigated in BDF1 male mice. Rosco was administered orally at ZT3 or at ZT19. We found that exposure to roscovitine was 38% higher and elimination half-life was 100% longer when dosing at ZT3 compared to ZT19. Moreover the tissue AUC/plasma AUC was higher at ZT3 in kidney, adipose, testis and lungs. The opposite was found in liver. *In vitro* microsomal assays indicated higher intrinsic clearance at ZT19. From these results, dosing times of roscovitine should be carefully considered in clinical trials.

Analytical method for the detection of N-&-N1 and CR8 using high performance liquid chromatography with UV detection (HPLC-UV) were developed and validated. The PK of both drugs was investigated in Balb/c mice. N-&-N1 showed higher potency in tumor cell death induction compared to roscovitine; however, N-&-N1 showed similar PK profile as roscovitine.

CR8 has 100% oral bioavailability, longer elimination half-life, rapid and extensive biodistribution. Systemic exposure higher than IC_{50} reported for cell death in tumor cell lines was achievable for more than 10 hr. These two analogues displayed favorable pharmacological properties, and thus are good candidates for further *in vivo* studies.

To conclude, these studies provide important knowledge about the PK, PD and PK/PD relationship of Rosco and its analogues. These studies may add more knowledge for treatment schedules and further preclinical and clinical development of Cdk inhibitors.

© Hatem Sallam

ISBN 978-91-7409-706-1

LIST OF PUBLICATIONS

- I. Song H, Vita M, **Sallam H**, Tehranchi R, Nilsson C, Sidén A, Hassan Z. Effect of the Cdk-inhibitor roscovitine on mouse hematopoietic progenitors in vivo and in vitro. *Cancer Chemother Pharmacol.* 2007, **60**: 841-9.
- II. **Hatem Sallam**, Patricia Jimenez, Hairong Songa, Marina Vita, Angel Cedazo-Minguez, Moustapha Hassan. Age-dependent pharmacokinetics and effect of roscovitine on Cdk5 and Erk1/2 in the rat brain. *Pharmacological Research.* 2008, **58**: 32–37.
- III. **Hatem Sallam**, Elisabeth Filipiski, Ylva Terelius, Francis Lévi and Moustapha Hassan. The effect of circadian rhythm on pharmacokinetics and metabolism of the Cdk inhibitor, roscovitine. (*Manuscript*).
- IV. Bettayeb K, **Sallam H**, Ferandin Y, Popowycz F, Fournet G, Hassan M, Echalié A, Bernard P, Endicott J, Joseph B, Meijer L. N-&-N, a new class of cell death-inducing kinase inhibitors derived from the purine roscovitine. *Mol Cancer Ther.* 2008, **7**: 2713-24.
- V. **Hatem Sallam**, Laurent Meijer and Moustapha Hassan. Quantitative analysis, pharmacokinetics and biodistribution of CR8, a new, roscovitine-derived, CDK inhibitor. (*Manuscript*).

Related publications not included in thesis

- I. Iurisci I, Filipiski E, **Sallam H**, Harper F, Guettier C, Maire I, Hassan M, Iacobelli S, Lévi F. Liver circadian clock, a pharmacologic target of cyclin-dependent kinase inhibitor seliciclib. *Chronobiol Int.* 2009, **26**: 1169-88

To my parents

CONTENTS

1.	Introduction	9
1.1	Cyclin dependent kinases	9
1.1.1	Regulations of Cdks	9
1.1.2	Functions of Cdks	9
1.1.3	The role of Cdks in disease	11
1.2	Cyclin dependent kinase inhibitors	13
1.2.1	Classification of the CdkI	14
1.2.2	(R)-Roscovitine (CYC202)	14
1.2.3	Effects of roscovitine	15
1.2.4	Pharmacokinetics and metabolism of roscovitine	20
1.2.5	Clinical trials of roscovitine	22
1.3	Second generation analogues of roscovitine	23
1.4	Role of Pharmacokinetics studies in drug discovery and development	24
1.4.1	Therapeutic drug monitoring	25
1.4.2	Age dependent pharmacokinetics	25
1.4.3	Population Pharmacokinetics	25
1.4.4	Chronopharmacology	26
1.5	Metabolism of xenobiotics	27
1.6	Development and validation of the bioanalytical methods	28
2.	General aims	29
3.	Materials and Methods	30
3.1	Materials	30
3.2	Animals	30
3.3	Treatment and sampling	31
3.4	Sample preparation	32
3.5	Analytical methods	33
3.6	Bioanalytical method validation	33
3.7	Clonogenic assays of the Hematopoietic progenitors	35
3.8	Western Blot	36
3.9	Pharmacokinetics analysis	36
3.10	In vitro metabolism of roscovitine	37
3.11	Statistical analysis	37
4.	Results	38
4.1	Preclinical pharmacokinetic and pharmacodynamic studies of roscovitine	38
4.1.1	PK and PD of roscovitine in the bone marrow in mouse	38
4.1.2	Age-dependent kinetics and dynamics of roscovitine in rat brain	42
4.1.3	Circadian rhythm-pharmacokinetics and metabolism of roscovitine	46
4.2	Second generation analogues of the cyclin dependent kinase inhibitors	49
4.2.1	N-&-N, a new class of kinase inhibitors derived from roscovitine	49
4.2.2	Pharmacokinetics and biodistribution of CR8	56
5.	Discussion	62
5.1	Myelosuppression	63
5.2	Age-dependent pharmacokinetics	65
5.3	Chrono-Bio-distribution	67
5.4	Roscovitine analogues	70
6.	Conclusions	73
7.	Future perspectives	74
8.	Acknowledgment	75
9.	References	79

List of abbreviations

ADME	Absorption, distribution, metabolism and elimination
ATP	Adenosine tri-phosphate
AUC	Area under the concentration-time curve
BFU-E	Burst-forming unit erythroid
CaM Kinase	Ca ²⁺ /calmodulin-dependent protein kinases
CK1	Casien kinase 1
Cdk	Cyclin-dependent kinase
CFU-GM	Colony-forming unit granulocyte-macrophage
CFU-GEMM	Colony-forming unit granulocyte-erythrocyte-monocyte-macrophage
Cl	Clearance
C _{max}	Maximum concentration
DMSO	Dimethyl Sulphoxide
DYRK1	Dual specificity tyrosine-phosphorylation-regulated kinase 1A
Erk	Extra-cellular regulated kinase
FAK	Focal adhesion kinase
GC	Gas chromatography
Gsk-3	Glycoken Synthase kinase 3
GIT	Gastro-intestinal tract
HCMV	Human cytomegalovirus
HIV	Human immunodeficiency virus
HPLC-UV	High performance liquid chromatography-Ultra-violet detector
IRAK-4	Interleukin-1 receptor-associated kinase 4
i.p.	Intra-peritoneal
i.v.	Intra-venous
IC ₅₀	Half maximal inhibitory concentration
LLOQ	Lower limit of Quantification
LOD	Limit of detection
NMDAR	<i>N</i> -methyl <i>D</i> -aspartate receptors
RB	Retinoblastoma
Roscovitine	(R)-roscovitine
T _{1/2}	Elimination half-life
Trail	Tumor necrosis factor-related apoptosis-inducing ligand
V _d	Volume of distribution

1. INTRODUCTION

1.1 CYCLIN DEPENDENT KINASES

Protein phosphorylation is a major post-translational process essentially involved in all intracellular regulatory pathways. Protein phosphorylation is catalyzed by protein kinases which phosphorylate the proteins on serine/threonine or tyrosine residues and the cellular ATP is used as a source of phosphate. The human kinome was found to consist of 518 enzymes[1].

Cyclin dependent kinases (Cdks) are a family of serine/threonine kinases that are activated through binding to a regulatory subunit called cyclins [2]. Cdk enzymes are homologues in a highly conserved "PSTAIRES" motif situated in their cyclin binding domain. Despite that the human sequencing program has succeeded in detection of 20 Cdks and 25 cyclins, still their functions is not fully understood and a limited number of active Cdks/cyclin complexes have been identified.

1.1.1 Regulation of Cdks

Cyclin dependent kinases are regulated by several mechanisms [2] including:

- 1- Transcription and translation of their subunits.
- 2- Heterodimerization with cyclins and formation of the Cdk/cyclin complex.
- 3- Post-translational modification by phosphorylation and dephosphorylation mechanisms. Phosphorylation at the thr14 and tyr15 by Wee1 and Myt1 enzymes inhibits the different Cdks, while the phosphorylation of thr160 by cyclin dependent kinase activating kinase complex (CAK, including Cdk7/cyclin H) is an activation step.
- 4- Interaction with the natural inhibitors such as Cip/Kip (p21, p27, p57) that inhibit the Cdks/cyclin complexes and INK4 proteins (p15, p16, p18 and p19) which inhibit the Cdk4 and Cdk6 monomers
- 5- Modification of Cdks cellular localization.

1.1.2 Functions of Cdks

1.1.2.1 Cell cycle control

Cdk/cyclin complexes play an essential role in the regulation of the cell cycle progression. Cyclin transcription and degradation occur during the different

phases of the cell cycle and lead to the activation or inactivation of the corresponding Cdks.

Transition between different phases of the cell cycle depends on the proper timely activated complexes specific for each phases. It has been shown that Cdk3/cyclin C is responsible for the exit of the cell from G₀ phase to start the G₁ phase. When Gap 1(G₁) phase starts, Cdk4 and Cdk6 couple with Cyclin D isoforms (D1-D3) and these complexes phosphorylate the retinoblastoma protein (Rb). Rb and other pocket like proteins function as transcription repressors through the binding of the E2F transcription factors. Phosphorylation of the Rb inhibits its activity and releases the E2F and activates the transcription of the necessary proteins for the DNA synthesis. In late G₁ phase, Cdk2 heterodimerize with Cyclin E and phosphorylate the Rb on additional sites. This further activates the transcription process and triggers irreversibly the gene expression of the S phase. This is called the G₁ phase checkpoint. Progression through the S phase is mediated by the Cdk2/cyclin A that further keeps the Rb hyperphosphorylated. In late S phase and in the beginning of G₂ phase, centrosome duplicates and migrates to form the poles of the mitotic spindle. This is mediated by both Cdk2/cyclinA and Cdk1/cyclin A [3]. Cdk1/cyclinA complex is also required for the transition from G₂ and commencement of mitosis phase (M) through regulation of chromosome condensation and microtubule dynamics. Progression through mitosis is mediated by the active Cdk1/cyclin B. At the end of mitosis Cdk1 activity is shut down by the degradation of Cyclin B by the anaphase promoting complex or cyclosome (APC-C) [2, 4, 5].

1.1.2.2 Transcription

Transcription is a multistep process including pre-initiation, initiation, promoter clearance, elongation, and termination. Cdks play very important roles in transcription initiation and elongation through the phosphorylation of the carboxyl terminal domain (CTD) of RNA polymerase II. Cdk7/cyclin H complex is a part of the transcription factor IIH (TFIIH) complex which phosphorylate the serine 5 residue of the RNA polymerase II. This step is necessary for the initiation of transcription. Cdk9/cyclin T forms the positive transcription elongation factor-b (P-TEFb). This complex phosphorylate serine 2 of the carboxyl terminal domain of RNA polymerase II and promotes the transcription

elongation [6, 7]. Cdk8/cyclin C has recently been found to play a role in the repression of transcription [8]. Cdk11 binds to cyclin L or D3 and plays a dual role in transcription [9].

1.1.2.3 Neuronal functions

Cdk5 has an essential role in the central and peripheral nervous system [10]. Cdk5 monomers as other Cdks are not active and need to bind to other regulatory units to be activated. Two of them have been identified as p35 and p39 [11, 12]. Other truncated forms of these proteins named p25 and p29 have been also identified [13].

Cdk5 regulates the cytoarchitecture of the developing brain [14] and mediates the neuronal migration in the post mitotic neurons. Cdk5 has also many important functions in the neuronal cytoskeleton dynamics, synaptic plasticity [15], drug addiction [16], synaptic endocytosis [17] and neurotransmitter release [18] and regulation of neuronal survival through the phosphorylation of the mitogen-activated protein kinases (MAPK) pathway [19, 20].

1.1.2.4 Cellular differentiation

Cdk5 was found to be a positive modulator of early myogenesis [21]. Cdk5/p35 also play important role in the differentiation of lens fibre cells. Cdk5 expression in HL60 leukemia cells induces the expression of CD14 and other monocytic cell morphology markers [14].

Also Cdk9 induces the differentiation in distinct tissue and it has been shown that the degree of expression of Cdk9 correlates with the degree of differentiation of primary neuroectodermal and neuroblastoma tumors [22].

1.1.2.5 Apoptosis

Cdk2 and Cdk5 have been shown to play different roles in induction and/or suppression of apoptosis in different tissues [23]. Cdk2 was found to regulate apoptosis in thymocytes [24]. Subcellular localization of Cdk2 have been found as a determinant of the apoptotic or proliferative fate of mesangial cells [25].

1.1.3 The role of Cdks in disease

During the past few years, the expression and/or activity of Cdks have been implicated in several diseases. The development of synthetic Cdk inhibitors would be an important strategy to treat such conditions.

1.1.3.1 Cancer

During the last decade it was established that the increase in expression and activity of different Cdks and cyclins in addition to the inactivation or decreased expression of the endogenous Cdk inhibitors may lead to high cell proliferation and inhibit the tight control of the cell cycle progression. The abnormal activity of Cdks allows the cells to escape from the different checkpoints including DNA damage checkpoint and to continue dividing in spite of their genomic instability. The inactivation of tumor suppressor genes, such as p53 or RB and/or genes encoding endogenous Cdk-inhibitors are the most frequent events occurring in malignant cells.

Over expression of cyclin B1 and hyperactivation of Cdk1 has been observed in a number of primary tumours including breast-, colon- and prostate carcinoma. Moreover, over expression of cyclin B1 was correlated with poor prognosis. Inactivation of Cip/Kip inhibitors and over expression of cyclin E and/or cyclin A lead to deregulation of Cdk2 in various malignancies, including melanoma, ovarian carcinoma (Cdk2/cyclin E), lung carcinoma (Cdk2/cyclin A) and osteosarcoma [26]. Hyper activation of Cdk4 and or Cdk6 may occur by over expression of cyclin D1 or inactivation of p16INK4A as found in parathyroid adenoma, leukemia, lymphomas, multiple myeloma and colorectal, gastric, kidney and breast cancer [27].

Cdk5 has been found to modulate the metastatic potential of some malignancies including breast and prostate carcinomas [28, 29]

1.1.3.2 Neurodegenerative disorders

Several studies have shown that deregulation of Cdk5 may be involved in the pathogenesis of several neurodegenerative disorders such as Alzheimer's disease, amyotrophic lateral sclerosis, Parkinson's disease and traumatic brain injury [10]. In neuronal cells, it has been shown that calpain might splice the p35 and lead to formation of shorter isoform called p25 [13]. This isoform is stable and leads to hyperactivation of Cdk5. Cdk5 has been shown to play an important role in the Tau protein phosphorylation [30]. In addition Cdk5 activation has been found to increase the brain tissue damage after acute brain injury as occurred in stroke or trauma accidents[31, 32].

1.1.3.3 Inflammation

Cdks play important role in the inflammation process. Cdk5 is catalyzing the GTP-dependent secretion in activated neutrophils [33]. Cdk4 and 6 appear to have roles in inflammatory cell differentiation, adhesion and recruitment as well as inflammatory cytokine production [34]. Cdk9 has also been shown to bind TRAF2, a protein that is involved in the activation of NF- κ B pathway mediated by the inflammatory cytokine TNF- α [35]. Moreover, several studies have suggested a relation between chronic inflammation and cancer induction where both infection and chronic inflammation contributes to 25% of all cancers. This might be due to genetic insult by the mediators of the inflammation like reactive oxygen species, different cytokines and growth factors [36].

1.1.3.4 Renal diseases

Phosphorylation of Rb protein by Cdk2 and subsequent release of the E2F transcriptional machinery has been implicated in cisplatin-related acute kidney injury. The E2F transcription factors was shown to induce the expression of pro-apoptotic proteins [37].

1.1.3.5 Infections

Cellular Cdks are also involved in replication of some viruses (e.g. CMV and HIV) [38-40] and in protozoal infections such as malaria and leishmaniasis [41].

1.2 CYCLIN DEPENDENT KINASE INHIBITORS

As mentioned previously, the activity of Cdks is tightly regulated in normal cells by different mechanisms. One of these mechanisms is the presence of natural inhibitors from the Cip/Kip and INK4 families. Due to the proven deregulation of the Cdks in different diseases including cancers, intensive efforts to find selective cyclin dependent kinase inhibitors (Cdk_i) has been conducted in the last 15 years. Several classes of different Cdk_i have been identified. In spite of their chemical diversity they share common characteristics [41]:

- (1) Cdk_i have low molecular weights (about 600).
- (2) Cdk_i are flat hydrophobic heterocycles.
- (3) Cdk_i act by competing with ATP for binding in the kinase ATP-binding site. No other type of inhibition has been identified.
- (4) Cdk_i bind mostly by hydrophobic interactions and hydrogen bonds with the kinase.

1.2.1 Classification of the Cdk

Cdk have been classified according to their selectivity into three groups:

1- Pan-cdk inhibitors that inhibit Cdk 1, 2, 4, 5, 6, 7 and 9 with almost similar potency like flavopiridol

2- Selective Cdk for Cdk 1, 2, 5, 7 and 9 such as the 2, 6, 9 tri-substituted purines olomoucine, roscovitine and purvalanol.

3- Selective Cdk for Cdk 4 and 6 such as PD-0332991 or P-276-00

1.2.2 (R)-Roscovitine (CYC202)

Roscovitine belongs to the 2, 6, 9 tri-substituted purines. It has been derived from olomoucine using classical medicinal chemistry and structure-activity relationship studies Figure 1 [4, 42]

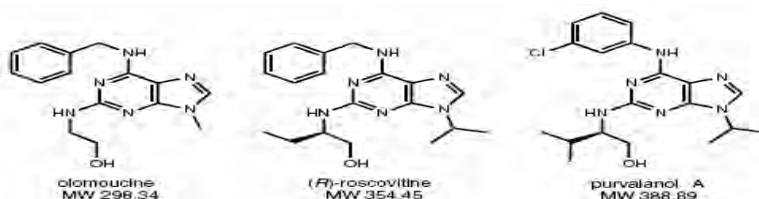


Figure 1: the structure of roscovitine and other members of the 2, 6, 9 trisubstituted Cdk

The inhibitory effect of roscovitine was tested using the kinase inhibitory assay on different kinase panels of total 151 kinases. Roscovitine was found to be rather selective on Cdk 1, 2, 5, 7 and 9 with the kinase IC₅₀ at the nanomolar range. Roscovitine was found to inhibit few other kinases such as CaM Kinase 2, CK1 α , CK1 δ , DYRK1A, EPHB2, ERK1, ERK2, FAK, and IRAK4 in the micromolar range (1-40 μ M). Most other tested kinases including Cdk4, Cdk6 and Cdk8 were insensitive to roscovitine. Another method was applied to test the selectivity of roscovitine. The method includes purification of roscovitine bound proteins by affinity chromatography followed by mass spectrometry for their identification. This method confirmed the selectivity profile of roscovitine; however it has also shown that roscovitine has bounded to pyridoxal kinase in all tested samples [43, 44].

The co-crystallization of roscovitine with Cdk2 and Cdk5 showed that the purine portion of the inhibitor binds to the adenine binding pocket of Cdk2. The

position of the benzyl ring of the inhibitor enables it for the contact with the enzyme. The purine ring was found to be located inside the ATP pocket of the kinase while the benzyl ring was found at C6 and thus to be out of the pocket. This is the opposite to the position of ATP complex where the purine ring lies outside the pocket and the phosphate groups are inside the pocket to allow the phosphorylation of the substrates [42].

Co crystal structure of roscovitine with pyridoxal kinase has recently been resolved. Surprisingly roscovitine was not bound to the ATP pocket of the enzyme. Instead it was bound to the pyridoxal (substrate) binding domain [44].

1.2.3 Effects of roscovitine

Effects of roscovitine have been studied in more than 100 cell lines. It has been shown that roscovitine acts through arrest of the cell cycle progression and induction of cell death. Within the study period, the cells did not develop resistance to roscovitine.

Since Cdks have an important role in wide range of cellular functions, roscovitine has been suggested as a potential treatment for several pathophysiologically different diseases. Roscovitine affects the cell cycle and apoptosis and thus may be implicated in the treatment of cancer.

1.2.3.1 Anti mitotic effects of roscovitine

Roscovitine arrests the cell division cycle in almost all the cell lines that have been studied. Different methods have been used to monitor the effects of the drug on cell proliferation including direct enumeration, FACS analysis, estimation of the number of viable cells and direct assay of DNA synthesis. Several studies have reported the IC₅₀ required to inhibit cell proliferation including NCI 60 cell line panel (average IC₅₀ = 16 µM) [4], the McClue et al. panel (19 cell lines; average IC₅₀ = 15.2 µM) [45], and the Raynaud et al. panel (24 cell lines; average IC₅₀ = 14.6 µM) [46]. The IC₅₀ average required for inhibition of cell proliferation in cancer cell lines does not exceed 17 µM.

Roscovitine was shown to be cell cycle phase non specific due to its ability for direct inhibition of of several Cdks (Figure 2A). Roscovitine inhibits the exit from G₀ (Cdk3/cyclin C), G₁/S transition (Cdk2/cyclin E), S phase progression (Cdk2/ cyclin A), G₂ phase (Cdk1/Cyclin A) and G₂/M transition (Cdk1/Cyclin B). The anti mitotic effect of roscovitine comprises combinations of these mechanisms. These effects depend also on the cycling status of the cells,

whether they are synchronized or not, the type of the cells and the exposure to roscovitine.

Indirect inhibition of the cell cycle by roscovitine is mediated through the inhibition of the activity of Cdk7/ cyclin H/ MAT1 (CAK). Inhibited CAK (Figure 2B) prevents the phosphorylation of the T loop threonine of various Cdks which prevents their activation and decreases activity of Cdk1, 2 and 4. Also phosphorylation of the inhibitor protein p27 by Cdk2 will be diminished [47] leading to its stabilization and more inhibition of the cell cycle [48].

In addition, roscovitine was shown to inhibit the initiation of DNA synthesis [49], the formation of centrosomes [50] and the formation of the nucleolus [51].

1.2.3.2 Cell death

Roscovitine has been shown to induce apoptotic cell death in several cell lines. The apoptotic features were confirmed by different biochemical and morphological markers. Roscovitine induced apoptosis regardless of the p53 status; however roscovitine has higher potency on wild type p53 cells compared to p53 null cells [4, 45, 52, 53]. Cell death was detected in all phases of the cell cycle.

Several studies have shown that different mechanisms including inhibition of the cell cycle due to p53 activation and inhibition of Cdk7/Cdk9-dependent transcription which inhibits RNA polymerase II enzyme might be involved in the induction of cell death [54, 55]. The effects of roscovitine on global transcription were shown to be rather limited and the expression of only few proteins was found to be severely reduced. This appears to be true for important survival factors such as Mcl-1; a member of the antiapoptotic Bcl-2 family, XIAP, and survivin. Induction of cell death by roscovitine thus seems to correlate rather well with inhibition of transcription of essential cell survival factors (Figure 2C). Furthermore, RNA polymerase II, as well as cyclin D1 and Cdk4 were decreased in HCT-116 and mantle cell lymphoma cell lines [53], [56].

Treatment with roscovitine has also been suggested to down regulate Chk1 and activate DNA damage response marked by an activation of ATM and Chk2.

Mcl-1 expression is strongly reduced in mantle cell lymphoma cell lines exposed to roscovitine [56]. The Mcl-1 down regulation by siRNA was found to

be sufficient to induce apoptosis in multiple myeloma cells [57]. Mcl-1 down regulation by roscovitine was also observed in multiple myeloma cells and in U937 monocytic leukemia cells [57, 58]. Roscovitine reduced the level of the antiapoptotic protein XIAP by down regulating XIAP mRNA expression [59]. On the other hand, down regulation of survivin and XIAP by roscovitine, was shown to contribute to the activation of caspases, and helped in overcoming glioma cell resistance to TRAIL-mediated apoptosis [60]. It also decreased the tyrosine phosphorylation and consequent activation of STAT5a, an upstream regulator of XIAP.

Alvi et al. has reported that roscovitine treatment of chronic lymphocytic leukemia (CLL) B-lymphocytes induced apoptotic cell death in significantly much higher level than in normal blood mononuclear cells, purified B-lymphocytes or purified T-lymphocytes. Roscovitine induced cell death in these cells was caspase-dependent but p53- independent and was accompanied with down regulation of Mcl-1 and XIAP [58].

1.2.3.3 Antitumor effects

The convergence of all the cellular effects of roscovitine explained earlier; provides the bases for explanation of the observed antitumor effects. The inhibition of cell cycle and the induction of apoptosis have rendered no cell line resistant to roscovitine effects until now [61].

Interestingly, tumor cells are more dependent on the short lived survival factors compared to normal cells and thus down regulation of these factors by roscovitine treatment has higher impact on tumor cells [62].

In addition, roscovitine has shown synergistic effect *in vitro* in combination with other chemotherapeutic agents such as camptothecin in MCF-7 breast tumor [63], irinotecan in p53-mutated colon cancer [64], histone deacetylase (LAQ824) in HL60 and Jurkat leukemic cells and doxorubicin in sarcoma cell lines [65]. Roscovitine showed also synergistic effect when combined with paclitaxel or cisplatin in human uterine sarcoma lines [66, 67].

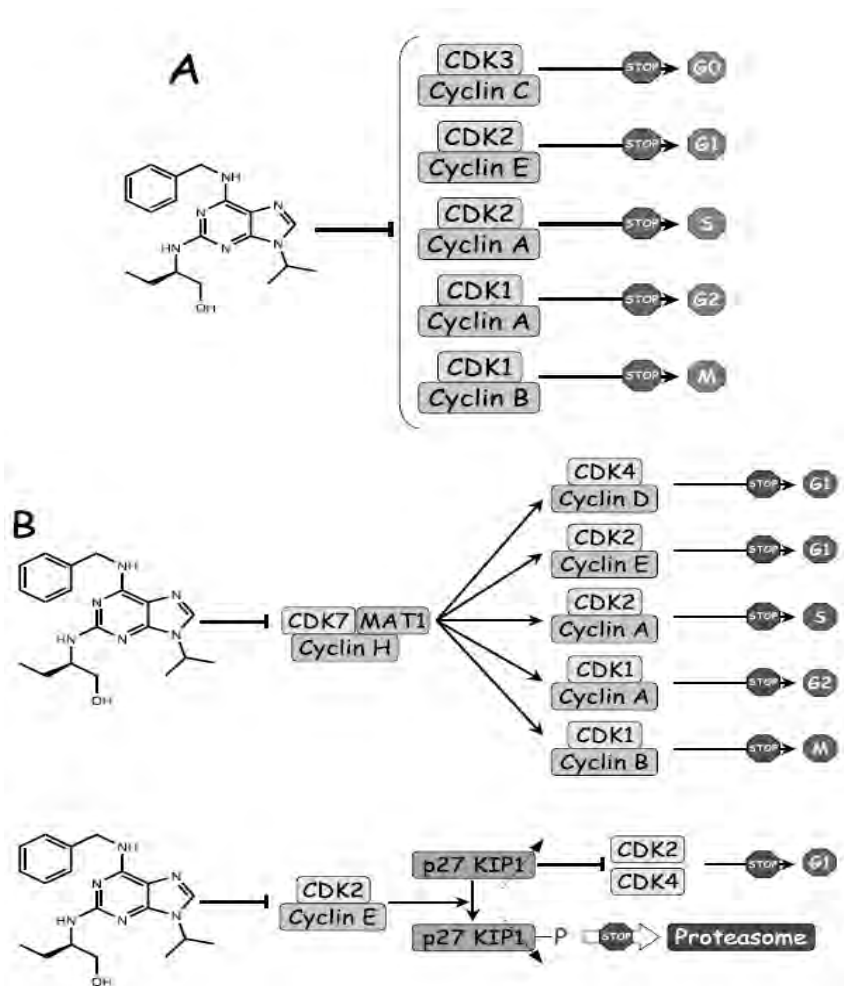


Figure 2. Multiple mechanisms of action of (R)-roscovitine and their cellular consequences.

(A) Direct interaction with Cdks leads to inhibition of the catalytic activity of various Cdk/cyclin complexes with a direct effect on various cell cycle phases (indicated by a "STOP" sign).

(B) Indirect inhibition of cell cycle progression: (i) interaction with Cdk7/cyclin H/MAT1 prevents the phosphorylation of a key activating threonine residue located on the T-loop of the substrate Cdks. Consequently, the activity of various Cdk/cyclin complexes is reduced; (ii) inhibition of Cdk2/cyclin E prevents phosphorylation and subsequent proteolytic degradation of p27KIP1, a natural Cdk2/Cdk4 inhibitor. p27KIP1 Accumulation thus contributes to an arrest in G1. (adopted from Meijer et al 2006) [62].

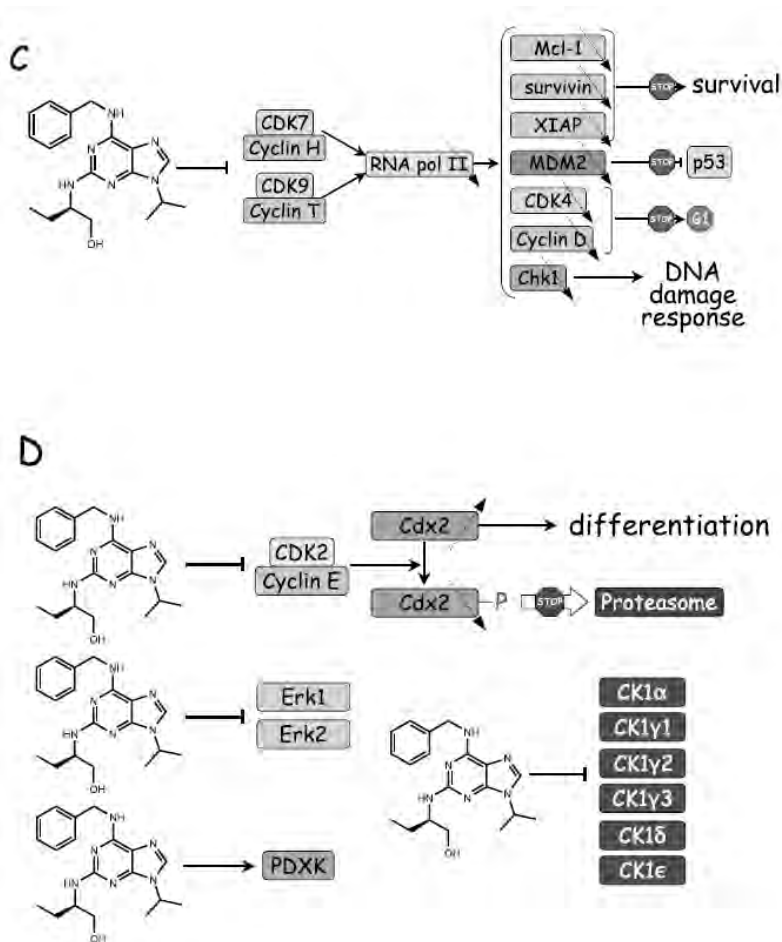


Figure 2. (C) Direct interaction with Cdk7/cyclin H and Cdk9/cyclin T leads to inhibition of RNA polymerase II (by lack of serine 2 and 5 phosphorylation). Consequently, transcription is reduced and short-lived proteins are rapidly downregulated. In particular, the reduction of survival factors such as Mcl-1, survivin, and XIAP contributes to cell death, the reduction of MDM2 level upregulates p53 level, reduced Cdk4 and cyclin D contribute to a G1 arrest, and downregulation of Chk1 leads to activation of a DNA damage response. Furthermore, Cdk7/Cdk9 inhibition by (R)-roscovitine leads to a down regulation of RNA polymerase II expression. (D) Other possible mechanisms of action. Inhibition of Cdk2/cyclin E prevents phosphorylation and subsequent proteolytic degradation of Cdx2, a transcription factor involved in intestinal cell differentiation. (R)-Roscovitine also inhibits the MAP-kinases Erk1 and Erk2, and members of the casein kinase 1 (CK1) family, contributing to its antiproliferative effects. Finally, (R)-roscovitine binds to pyridoxal kinase (PDXK). adopted from Meijer et al 2006)[62]

Roscovitine has been studied in various tumor xenografts models. McClue et al. studied antitumor effect of roscovitine in human colorectal and uterine cancer xenografts. Nude mice bearing Lovo human colorectal tumor were treated with roscovitine i.p. in a dose of 100 mg/kg x3 times daily for 5 days.

Roscovitin induced 45% reduction in tumor volume compared to the controls and 58% reduction in tumor weight compared to the controls (T/C). The second xenografts model was nude mice bearing human uterine xenograft MESSA-DX5. Roscovitin was administered orally (500 mg/kg x 3 daily) for 4 days. Roscovitin inhibited the tumor growth rate by 62% compared to the controls and the T/C value was 47% [45]. Raynaud et al. have reported that roscovitin administered orally (500 mg/kg bid) for 5 days has reduced the tumor weight compared to controls by 75% in nude mice bearing HCT116 tumor xenografts [53].

Lurisci et al reported the efficacy of roscovitin in non nude mice bearing tumor xenografts. BDF1 male mice bearing Glasgow osteosarcoma xenografts were treated with roscovitin orally (300 mg/kg x1 daily) for 5 days. The drug was administered at Zeitgeber time 3 (ZT3, 3 hours after light onset) or at ZT11 or ZT19. Roscovitin reduced the tumor growth by 35% when administered in the active time of the mice (ZT19) and 55% when administered during their rest span (ZT3 or ZT11) [68]. Roscovitin was also shown to be effective in reducing the growth of A4573 (Ewing's sarcoma) and PC3 prostate tumor xenografts [52, 69].

Roscovitin showed higher anti tumor activity in combination with other antitumor treatments. Maggiorella et al has reported better reduction in tumor volume from 54% to 72% when a single dose of roscovitin 100 mg/kg was given i.p. and combined with radiation therapy in mice bearing MDA-MB 231 (breast cancer) [70]. Roscovitin was shown to have synergistic effect in inhibiting HT29 colon cancer xenografts when combined with irinotecan [64].

1.2.4 Pharmacokinetics and metabolism of roscovitin

Pharmacokinetics (PK) of roscovitin was reported in mice, rats and human. Vita et al. reported the PK and biodistribution of roscovitin in rats after a dose of 25 mg/kg. Roscovitin PK was described by a two-compartment open model and biphasic elimination. The elimination half-life was rapid (<30 min). The highest exposure to roscovitin was observed in lungs followed by liver, fat and kidney. Roscovitin concentration in the brain was 30% of that observed in plasma. Vita et al. have also identified three major metabolites. However, no metabolites were detected in brain [71, 72].

Pharmacokinetic of roscovitin were investigated in BALB/c and Tg26 mice.

These studies showed rapid and biphasic clearance of roscovitine from plasma following i.v., i.p. or oral administration [53, 73, 74]. Roscovitine had rapid tissue distribution and rapid elimination with a half-life of 1.19 hr. Plasma concentrations above 15 μM (the average IC₅₀ values obtained with various tumor cell lines) were observed for 4, 12, and 24 h following oral administration of 50, 500, and 2000 mg/kg, respectively [53].

The pharmacokinetics of roscovitine in humans were reported in two phase-I trials, the first one was conducted in healthy volunteers. Roscovitine was administered orally as a single dose of 50, 100, 200, 400, and 800 mg and the concentrations of roscovitine and its carboxylated metabolite were followed in plasma and urine. Roscovitine was found to undergo slow absorption from the GIT but it was rapidly and extensively distributed into the tissues. Roscovitine was found to have rapid metabolism and non-saturated high protein binding. Moreover, food intake didn't affect the bioavailability of the drug [75].

In the second investigation, twenty-one patients with a median age of 62 years (range: 39–73 years) were treated with roscovitine in doses of 100, 200 and 800 mg twice daily for 7 days. At 800 mg b.i.d. roscovitine reached peak plasma concentrations at 1- 4 hr and the elimination half-life ranged between 2–5 hr depending on the dose. Interestingly, the inhibition of retinoblastoma protein (RB) phosphorylation was not found in peripheral blood mononuclear cells. RB phosphorylation was suggested as a suitable PD endpoint [76].

Roscovitine was shown to have high protein binding in human and mice plasma ranging from 92% to 96% [53, 77].

In vitro and *in vivo* metabolism of roscovitine was reported recently [78]. *In vitro* metabolism was examined using liver microsomes prepared from different animal species and from human livers. Several metabolites were identified including the carboxylate metabolite (oxidation of the alcohol group at C2 of the purine ring) [72]. McClue et al. have shown that CYP3A4 and CYP2B6 enzymes are the main enzymes for roscovitine metabolism in human microsomes. Roscovitine was found to undergo phase II metabolism through conjugation with glucuronic acid by the phase II UGT1A3, 1A9 and 2B7.

In vitro assays also showed that roscovitine was able to inhibit its own metabolism through inhibition of CYP3A4. The IC₅₀ for enzyme inhibition was as low as 3.2 μM . However, the authors reported also unpublished data about the *in vivo* induction of roscovitine metabolism and raised the question about

possible drug-drug interactions which might be detected in the clinic. These results were in accordance with the previous published data concerning roscovitine metabolism [72, 74, 79].

1.2.5 Clinical trials of roscovitine

Phase-I trials of roscovitine has been conducted in healthy volunteers and advanced malignancy patients and the PK results are discussed above.

These studies also reported a good tolerability profile of roscovitine. Dose-limiting toxicities (DLT) were seen at the 800 mg twice daily and included grade 3 fatigue, grade 3 hyponatraemia, grade 3 skin rash, grade 4 hypokalaemia, grade 2 reversible raised creatinine, reversible grade 3 abnormal liver function and grade 2 emesis [76].

Although the efficacy of roscovitine was not the main concern in these trials, the antitumour activity was monitored in a total of 70 patients. One patient with hepatocellular carcinoma showed partial response (PR) and 10 patients showed stable diseases (SDs) lasting for > 4 months, two of these patients were diagnosed non-small cell lung cancer (NSCLC), the disease stabilization in these patients lasted for more than 1 year [80].

Currently roscovitine has entered phase IIb clinical trials in advanced non-small lung cancer and naso-pharyngeal cancer. Roscovitine was also tested in phase-II clinical trials as single agent in hematological B-cell malignancies and in combination trials with gemcitabine/cisplatin as first-line treatment of NSCLC, with docetaxel in second line treatment of NSCLC and with capecitabine in metastatic breast cancer. Phase-I trials of roscovitine in the treatment of glomerulonephritis are ongoing.

In summary, until now the antitumor activity of roscovitine in cancer patients was shown to be modest and below the predicted efficacy from the preclinical studies. These unexpected results have raised a major concern about the PK profile of roscovitine in man. Roscovitine was rapidly eliminated and its concentrations above the target levels were not sustained.

1.3 SECOND GENERATION ANALOGUES OF ROSCOVITINE

The antitumor efficacy of roscovitine was questioned due to the following reasons:

- 1- Short half-life and rapid metabolism to inactive metabolites.
- 2- Rather weak potency on Cdks (submicromolar range) and tumor cell lines (micromolar range).
- 3- The need for high doses in clinical trials to detect reasonable effect.

All these factors have raised the interest in synthesis and optimization of second generation analogues of roscovitine. These analogues should have higher potency of Cdks inhibition, tumor growth inhibition, better PK profile with longer elimination half-life, better distribution and better oral bioavailability and lastly good tolerability and safety profile.

Active and intensive research efforts to synthesize these analogues and to test their biological effects are being currently conducted by Dr. Laurent Meijer and his group at Roscoff, France [43, 81-83]. This research combines the empirical medicinal chemistry approaches with the reported information about the co-crystal structure of roscovitine with different Cdks and the information about roscovitine metabolism.

Recently the synthesis and biological characterization of CR8, a second generation analogue of roscovitine was reported [83] Figure 3. The synthesis of CR8 was done by the manipulation of the substitution at C6 of the purine ring which is not reported to be catalyzed in the metabolism of roscovitine [53, 72]. Bettayeb et al. have shown that the in vitro IC₅₀ of CR8 needed to obtain a desirable pharmacological effect on different tumor cell lines were about 0.7 μM [81] which is 50-100-fold below that reported for roscovitine [62].

Still the pharmacokinetic and safety profile of CR8 and other perspective analogues need to be analyzed as early as possible prior to further preclinical and possibly clinical investigations [84].

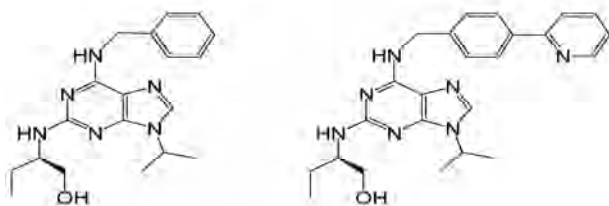


Figure 3. The chemical structure of (R)-roscovitine and (R)-CR8.

1.4 ROLE OF PHARMACOKINETICS STUDIES IN DRUG DISCOVERY AND DEVELOPMENT

Research for new drugs until clinical approval usually proceeds in 2 stages; drug discovery stage and drug development stage.

In drug discovery stage scientists are working to set up a working hypothesis of the target enzyme or receptor for a particular disease, to establish suitable models and to screen the new drug molecules for *in vitro* and/or *in vivo* biological activities. In the development stage, the new drug candidates are evaluated for their toxicity and efficacy [84].

It is estimated that approximately 10 -40 % of drug research programs fail due improper pharmacokinetic properties. Drug metabolism and pharmacokinetics (DMPK) studies became an essential part in any drug discovery and development programs and are usually preformed as early as the start of biological activity screening.

In drug discovery phase, early DMPK screening provides a risk assessment against the most likely reasons for failure in the drug development phase. Also it provides crucial information for assessing the pharmacokinetic structure–activity relationships of the new candidates. This information is important for the lead optimization efforts.

In drug development phase, DMPK studies provide vital information about the PK/PD relationship and the possible PK/PD mismatch (i.e., duration of action shorter or longer than predicted from the drug half-life) [85]. This information is relevant to select the dosing schedules which will be implied for first time in human studies [86] and to establish the early predictions of the clinically effective dose.

The following tests could be implied in the DMPK studies[84]:

- 1- *In vitro* metabolic assays using liver microsomes, recombinant enzymes or cultured hepatocytes.
- 2- Inhibition or induction of liver metabolizing enzymes.
- 3- *In vitro* tissue penetration assays.
- 4- PK studies in animal models during preclinical drug evaluation.

PK is the key for right dosing of drugs in the clinical settings, different examples of its uses are highlighted below.

1.4.1 Therapeutic drug monitoring

The use of pharmacokinetic (PK) parameters to individualize treatment is a powerful tool used mainly for drugs with narrow therapeutic window like anti-cancer agents e.g. busulphan [87] and immunosuppressants e.g. cyclosporine and sirolimus. Other drugs like theophylline and digoxin are examples of drugs in which drug monitoring for pharmacokinetic-directed therapy (PKDT) is routinely performed. The need for therapeutic drug monitoring (TDM) in such highly toxic agents arises from the high inter-individual and intra-individual variability in PK. Using fixed dosing schedules for these agents may result in either sub-optimal or toxic exposure. TDM to a fixed PK endpoint can be done reliably due to the recent advances in determination of drug metabolism, active metabolites if present, and the ability to measure drug concentrations [88, 89].

1.4.2 Age dependent pharmacokinetics

The age is one of the important factors affecting the PK and efficacy of the drugs. Variability in drug exposure and efficacy occurs among the different age populations i.e. children, adults and elderly. It is essential to investigate the PK parameters in the age population that is treated with the drug. In the young age population like neonates and infants, doses of many drugs is still not optimized due to lack of knowledge about drug disposition and PK in this population. Several factors such as the ontogeny of the metabolizing enzymes and drug transporters are responsible for variability of drug metabolism and PK [90]. Continuous efforts are being done to develop accurate PK models to predict the PK parameters in this population without conducting large scale investigation which might be difficult due to technical and ethical restraints [91]. Examples of trial efforts in human include: using population pharmacokinetic studies, allometric scaling of drug disposition according to body weight and *in silico* prediction of pharmacokinetics [90].

Another approach may be the implication of age dependent pharmacokinetics and toxicokinetics in young animals during different stages of drug development [92].

1.4.3 Population Pharmacokinetics

Population pharmacokinetic (PPK) is a science which investigates pharmacokinetics in special populations such as neonates, the elderly, patients

with AIDS, critical care patients, and those with cancer. PPK play a pivotal role in direct patient care by having a high degree of utility for the construction of patient dosing strategies. PPK is valuable because it targets the patient group that will receive the drug of interest, quantify pharmacokinetic variability and try to explain those sources of variability [93].

1.4.4 Chronopharmacology

The circadian timing system functions to optimize the metabolism and energy utilization for the processes necessary to sustain life. Most of the physiological processes follow a circadian rhythm, e.g. heart rate, blood pressure, urine production, intestinal peristalsis, adrenal corticosteroids secretion, xenobiotics metabolism, liver and renal blood flow and secretion of digestive enzymes [94, 95].

The circadian rhythm is produced in the cells through the molecular clock which is composed of 12 clock genes. The molecular clock has positive limb composed of CLOCK, NPAS2 and BMAL1 genes and negative limb composed of PER1, PER2 and CRY genes with feedback loops in between including the orphan gene REV-ERB α . The oscillations in the transcription and translation of the molecular clock genes produce the circadian rhythm. The orchestration of the circadian rhythm in the peripheral tissues in mammals is maintained by the Supra-Chiasmatic nucleus (SCN) at the anterior hypothalamus. The SCN is synchronized mainly by the light-dark cycles; however peripheral tissue can be synchronized with the food-fasting cycles [95, 96].

The disruption of circadian rhythm has been found to accelerate the tumor growth in experimental animals and cancer patients and has bad implications on their prognosis [96-99].

Due to the rhythmic regulation of most of the physiological processes controlling the detoxification of xenobiotics, it has been found that the time of dosing can modify significantly the pharmacokinetics of drugs, the study of such circadian time dependence is called **chronopharmacokinetics** [100]. Also such dependence on dosing time for the **chronopharmacodynamics** of the drugs and their therapeutic value with best efficacy and maximum tolerance has been documented for many drugs such as anticancer drugs irinotecan, 5-fluoruracil and oxaliplatin among others [101-103].

Optimization of the dosing time for the drugs is called **chronotherapeutics** which has been implemented for several classes of drugs including anticancer, cardiovascular, respiratory, anti-ulcer, anti-inflammatory, immunosuppressive and antiepileptic drugs (Figure 4) [94, 104, 105].

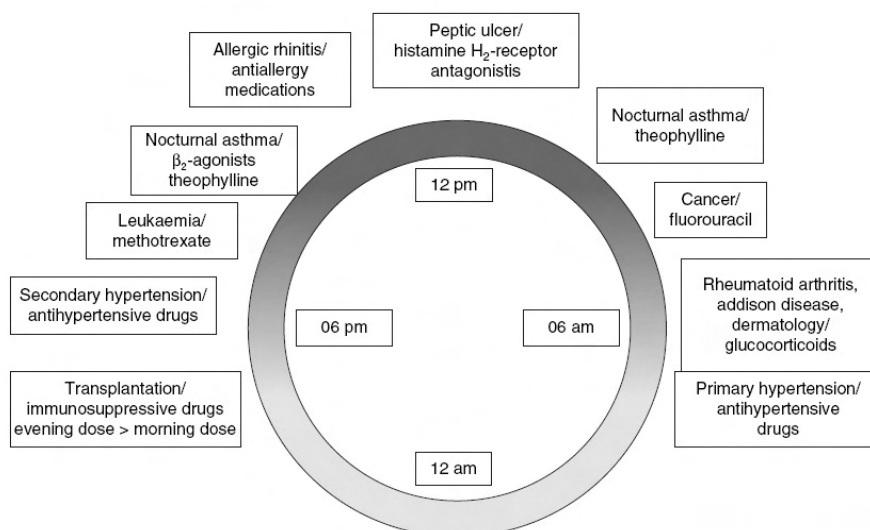


Figure 4: examples for application of chronopharmacology in man. Diseases and relative recommended administration time for drugs according to reported knowledge. (adopted from baraldo et al., 2008)[94]

1.5 METABOLISM OF XENOBIOTICS

Hydrophilic compounds are usually eliminated through the renal excretion. That is not optimally achievable in the lipophilic compounds, which are eliminated through the process of biotransformation. Metabolic biotransformation is mediated by the metabolizing enzymes mainly located in the liver. However small portion of the xenobiotic metabolism is mediated by metabolic enzymes in the intestine and kidney.

Metabolic biotransformation usually advances through 2 phases:

Phase I reactions: usually convert the parent drug to a more polar metabolite by introducing or unmasking a functional group like ($-OH$, $-NH_2$, $-SH$). Phase I metabolites are usually inactive, although in some cases they may be more active or toxic.

Phase II reactions: they are conjugation reactions in which the phase I metabolites might be conjugated to endogenous substrate such as glucuronic

acid, sulfuric acid, acetic acid, or an amino acid to form a highly polar compounds

The cytochrome P-450 (CYP) family of enzymes are a large group of hemoproteins located in the endoplasmic reticulum of the hepatocytes, lung, intestine and the brain [106]. They are mainly responsible for oxidative metabolism of many drugs, steroids, and carcinogens [107].

CYP enzymes are one of the major determinants of inter-individual and intra-individual variability in human PK. Inter-individual variability could arise from the genetic polymorphism of different enzymes. Individuals are classified according to their enzymatic metabolic activity to low-, rapid- or ultra rapid- metabolizers [108]. Intra individual variability could be attributed to the inhibition or induction of the enzymes by the substrates. Also circadian fluctuation in CYP enzymes or their protein partners as P450 oxidoreductase which provide the electrons necessary for the CYP functions expression and activity might contribute to this type of variability [95, 109].

1.6 DEVELOPMENT AND VALIDATION OF THE BIOANALYTICAL METHODS

The quantitative determination of drugs and their metabolites in biological samples are the key method needed to generate the required data for PK modeling [110]. For this purpose the development and validation of accurate analytical methods for drugs are the first step done in the DMPK studies. Modern drug analysis implements different instruments like high performance liquid chromatography (HPLC), gas chromatography (GC), liquid chromatography-mass spectrometry (LC-MS), liquid chromatography-tandem mass spectrometry (LC-MS-MS) and ligand- based assays (such as RIA and ELISA) [111].

The analytical methods need to be validated to assure both accuracy and reproducibility. Bioanalytical method validation includes all of the procedures required to demonstrate that the quantitative determination of the concentration of an analyte in a particular biological matrix is reliable for the intended application. FDA has set up guidelines for the bioanalytical method validation which are obligatory to be reported in any drug approval application [112].

The validation criteria are explained in details in the materials and methods section.

2. GENERAL AIMS

The overall aim of the present thesis was to investigate the pharmacokinetics, chronopharmacokinetics and pharmacodynamics of the Cdk inhibitors; roscovitine and new analogues in preclinical animal models. Thus this knowledge may help in the proper design and optimization of dosing regimens in clinical trials.

Specific aims

- To study the biodistribution, pharmacodynamics and toxicity of roscovitine on the murine hematopoietic progenitors *in vitro* and *in vivo*.
- To study the age-dependent pharmacokinetics of roscovitine in rats and to determine its effects on the Cdk5 and Erk1/2 in the brain.
- To study the effect of circadian rhythm on the pharmacokinetics, biodistribution and metabolism of roscovitine.
- To assess the biochemical activity and anti tumor efficacy of N-&-N1; a new analogue of roscovitine. To develop and validate bioanalytical method for N-&-N1 and to study the pharmacokinetics of N-&-N1 in female Balb/c mice.
- To develop and validate bioanalytical method for CR8; a second generation analogue of roscovitine and to investigate its bioavailability, pharmacokinetics and biodistribution.

3. MATERIALS AND METHODS

3.1 MATERIALS

Chemicals

Roscovitine was purchased from LC Laboratories (USA). (S)-CR8 was synthesized as described previously (Oumata et al., 2009). Tetrahydrofuran, methanol, acetonitrile and DMSO (HPLC grade) were obtained from Merck (Darmstadt, Germany) and Sigma-Aldrich (Stockholm, Sweden). Heparin (5000 IU/ml) was obtained from LeoPharma A/S, Ballerup, Denmark. All other reagents and solvents were of HPLC analytical grade. Chemiluminescence reagents (ECL) from (Amersham Pharmacia Biotech, UK)

Pooled plasma from healthy donors was obtained from the Blood Transfusion Center, Karolinska University Hospital. Stock solutions of roscovitine, S-CR8 and N&N1 were prepared in DMSO. Serial dilutions in Methanol or 50mM HCl were prepared from the main stock for the calibration curves, quality control samples and doses for administration to the animals. All stocks and standards were stored at -20 °C.

Antibodies

Cdk5-p35 antibodies (C19) were purchased from Santa Cruz Biotech Inc. (Santa Cruz, CA, USA), Beta-actin antibodies were purchased from Sigma (St. Louis, MO, USA) and pErk1/2 antibodies were purchased from Cell signaling technology (Beverly, MA, USA). Horse raddish peroxidase-conjugated anti rabbit and anti mice secondary antibodies (Amersham Pharmacia Biotech, UK).

Media

RPMI 1640 medium, Phosphate-buffered saline (PBS), Iscove's modified Dulbecco's medium (IMDM), Foetal bovine serum (FBS) from Invitrogen AB (Stockholm, Sweden); Methocult GF M3434, MethoCult M3534 and MethoCult M3334 from Stem Cell Technologies Inc. (Vancouver, Canada).

3.2 ANIMALS

All experiments described herein were approved by the regional ethics committee for animal research in accordance with the Animal Protection Law, the Animal Protection Regulation and the Regulation for the Swedish National Board for Laboratory Animals.

Female Balb/c mice aged 8-12 weeks (study I, IV and V), Sprague-Dawley Pregnant female rats, 14 days rat pups and adult male rats (200-250g) (study II)

were obtained from B&K laboratories and Scanbur (Sweden). In study III B2D6F1 (8-10 weeks old) male mice were purchased from Janvier (Le Genest St Isle, France).

All animals were allowed to acclimatize to their surroundings for one week before starting the treatment. They were kept under controlled conditions of temperature, relative humidity and 12 h daylight cycle and were fed standard pellet and water ad libitum.

3.3 TREATMENT AND SAMPLING

Study I: For pharmacokinetics analysis Roscovitine in DMSO was further diluted with sodium chloride 9 mg/ml (1:9 v/v) and immediately administered intraperitoneally (i.p.) to the animals in a dose of 50 mg/kg. Blood and bone marrow were sampled at 10, 20 and 30 minutes and 1, 2, 3, 4, 6 and 8 hours. Two animals were used for each time point.

For hematopoietic toxicity study, roscovitine was administered i.p. as a single dose of 50, 100 or 250 mg/kg or as a multiple doses schedule of 350 mg/kg/day divided in two daily doses for four consecutive days.

Study II: Adult rats and rat pups were injected i.p. with a single dose of roscovitine (25 mg/kg) dissolved in DMSO/saline (10/90, v/v). Animals were divided into 2 groups, one for roscovitine pharmacokinetics study and the others for the western blotting.

The olfactory bulb was removed and the brain was divided into two hemispheres. The brains were then dissected into frontal cortex, (FC), hippocampus (HC), and cerebellum (CR). The different regions were immediately frozen to -70 °C until assay. Heparinized blood was collected by cardiac puncture at the given time points,

Study III: Roscovitine was administered as a single oral dose (300mg/kg dissolved in 50mM HCl) to male BDF1 mice. The drug administration was carried out at ZT3 or ZT19 (ZT – Zeitgeber Time is the number of hours after light onset). Blood was collected at 10, 20, 30 min and 1, 2, 4, 6, 8, 12 and 24hr. Organs were removed, weighted carefully and frozen until analysis.

Study IV: Female Balb/c mice were administered a single i.p dose of N&N1 (25mg/kg dissolved in DMSO:NaCl 10:90 v:v). Blood samples were collected by cardiac puncture in heparinized tubes 10, 20, 30, 45, and 60 min and 2, 3, 4, 6, and 7 h after administration.

Study V: Two groups of female Balb/c mice were treated with S-CR8 dissolved in 50mM HCl. One group was administered the drug i.v. in a dose of 50mg/kg. The

second group received the drug orally in a dose of 100mg/kg. Blood samples were collected by cardiac puncture into heparinized tubes at 10, 20, 30, 60 min, 2, 4, 6, 8 h post administration. Organs were collected and snap frozen in liquid nitrogen to avoid any metabolic activities until samples storage at -20°C

Control animals were administered the drugs vehicles in all the studies. Plasma was separated by centrifugation at 3000×g for 5 min and stored in -20 °C until analysis.

3.4 SAMPLE PREPARATION

For chromatographic analysis

Plasma samples: For roscovitine samples; plasma proteins were precipitated using acetonitrile at a ratio of 1:1 v:v, while for S-CR8 and N&N1; plasma proteins were precipitated with methanol at a ratio of 1:2 v:v. Samples were vortexed for 30 sec and centrifuged at 10000 rpm for 10min. Fifty µl from the supernatant were injected into the HPLC.

Organs: Pre-weighted organs were placed in 0.9% NaCl (1:3 – 1:5 ratio, w/v). Samples were homogenised by probe sonication between 1 min and 3minutes, depending on the tissue type. After sonication, acetonitrile or methanol was added at ratio of 1:2 w:v except for the brain, acetonitrile was added at ratio of 1:1.

Samples were vortexed vigorously, centrifuged at 10000 rpm for 15min and fifty µl from the supernatant were injected into the HPLC. Organs concentrations were calculated back to µg/g tissue.

Western blot

The brain tissues from different brain parts of the control and treated animals were homogenized by sonication in ice-cold isolation buffer (RIPA) containing protease cocktail inhibitors (1:500), and phosphatase cocktail inhibitors (1:100). The homogenate was centrifuged at 14,000rpm for 15min at 4 °C to eliminate cellular debris and the protein content was determined using Bradford method.

Bone marrow

Bone marrow from both femurs was flushed out with 0.15 ml of sodium chloride (9 mg/ml). single-cell suspension was prepared by gentle flushing through needle and syringe. Nucleated cells were counted using Türk solution and bone marrows were stored at -20°C until assay.

3.5 ANALYTICAL METHODS

Chromatographic analysis utilizing high performance liquid chromatography with UV-detector (HPLC-UV) was used to detect and quantify the 3 cyclin dependant kinases inhibitors (roscovitine and its new analogues, S-CR8 and N&N1)

High performance liquid chromatography (HPLC-UV)

The HPLC-UV system consisted of a Gilson 234 auto-injector equipped with a 100 µL loop, an LKB 2150 pump (Pharmacia inc., Sweden), an “LDC analytical spectro-monitor 3200” UV-detector (USA) and a CSW 32 chromatography station integrator.

Roscovitine (Study I, II and III) was analyzed as described previously with minor modifications (vita et al 2004). Separation was performed on a Zorbax SB C18 column (3.5 µm x 4.6 mm x 75 mm) from Agilent (USA). The mobile phase consisted of tetrahydrofuran: 0.1% phosphoric acid (25:75), the flow rate was 0.9 ml/min, and the analysis time was 6min. The UV wavelength used was 292 nm.

S-CR8 (study V) was separated on a Zorbax SB-CN column (3.5 µm x 4.6 mm x 150 mm) from Agilent (USA). The mobile phase consisted of tetrahydrofuran: 25 mM phosphate buffer pH = 2.6, ionic strength = 0.022 (20:80, v/v). The flow rate was set at 0.9 mL/min, running time at 8 min for standard curve and quality controls and at 15 min for animal samples to elute all the metabolites. Injection volume was 50 µL and the UV wavelength used was 305 nm. Standard curves were prepared from spiked pooled human plasma. The calibration curve was linear within the range 0.1 to 10 µg/mL.

N-&-N1 (study IV) analysis was performed on a Zorbax SB C18 column (3.5 µm x 4.6 mm x 75 mm) from Agilent (USA). The mobile phase consisted of tetrahydrofuran: phosphoric acid 0.1% in water (16:84, v/v). Flow rate was set at 1 mL/min, running time at 25 min and injection volume was 50 µL. The UV wavelength used was 220 nm. Standard curves were prepared from spiked pooled human plasma, and were linear within the range 0.1 to 5 µg/mL.

3.6 BIOANALYTICAL METHOD VALIDATION

Validation of the quantitative analytical methods was carried out according to the FDA bioanalytical assay validation guidelines as reported by Shah et al.

1- Selectivity

Selectivity of the HPLC analysis was confirmed by absence of no interfering peaks in the blank biological samples from untreated animals and animals receiving only the drug vehicle.

2- Calibration curve

Calibration curves for all the studied compounds were constructed from at least eight standard points of different concentrations ranging either from 0.1 to 5 µg/ml for roscovitine and N&N1, or from 0.1 to 10 µg/ml for S-CR8. The peak areas were plotted against the concentrations. Linearity was assessed by a weighted least-squares regression analysis and the correlation coefficient (r^2) of 0.99 or better was acceptable. The lower limit of quantification (LLOQ) was set as the lowest measurable concentration with acceptable accuracy and precision not more than 20% [113].

3- Precision and accuracy

The precision of the method was defined as the percent relative standard deviation (% SD) calculated from triplicate measurements [(standard deviation)/mean value] × 100 and the accuracy was defined as the percent relative error of the mean(% SEM) of the replicate measurements from the theoretical values [(measured value - nominal value) /nominal value] × 100 [113, 114]. Precision and accuracy were determined by analyzing quality control samples (QCs) prepared at four concentrations (0.75, 1.5, 3.5 and 7.0 µg/mL) with pentaplicates on three consecutive days [112].

4- Recovery

Absolute recovery is defined as percentage of reference compound that is measured to that the exact amount of compound added to a blank buffer [111]. Recovery is computed by comparing responses of triplicates of extracted middle QC (1.5 µg/mL) samples with those of extracted blank matrix to which CR8 has been added at the same nominal concentration [110].

Relative recovery is defined as percentage of the amount of drug measured from the plasma to the amount measured from pure solvent (e.g. 50 mM HCL) [111]. The medium controls (1.5 µg/mL) were prepared in normal plasma and

50mM HCl. Samples were run in triplicate and recovery was calculated as the percentage of (plasma peak area/methanol peak area) x 100.

5- Stability

Stability of N&N1 and S-CR8 (study IV and V) was determined. QC Samples were kept at room temperature, +4 °C and at -20 °C and analyzed twice weekly for 2 months. Peak areas of all the samples were compared to the peak areas obtained at time zero.

3.7 CLONOGENIC ASSAYS OF THE HEMATOPOITIC PROGENITORS

The effect of roscovitine was investigated on the clonogenic capacity of the hematopoietic progenitors in the bone marrow both *in vitro* and *in vivo*.

For *in vitro* study:

1- Nucleated marrow cells from untreated female Balb/c mice were incubated with roscovitine in IMDM supplemented with 20% FBS (IMDM/FBS) before plating in MethoCult media.

2- After that nucleated marrow cells from untreated female Balb/c mice were plated in 1.1 ml MethoCult medium with or without roscovitine (1, 10, 25, and 100 µMol) in 35 mm Petri dishes in duplicates. Dishes were incubated at 37°C with 5% CO₂ and 95% humidity.

Colonies were scored using an inverted microscope. CFU-GM colonies were defined as consisting of 50 or more cells, and BFU-E as consisting of 30 or more cells.

Twenty thousand nucleated cells in MethoCult M3534 and 2×10^5 nucleated cells in MethoCult M3334 were plated and scored at day 7 for CFU-GM and BFU-E, respectively. Twenty thousand nucleated cells were plated in MethoCult M3434 and scored for CFU-GM, BFU-E and CFU-GEMM on day 12. DMSO concentrations in all samples were 0.3%

For *in vivo* study

Female Balb/c mice treated with a single or multiple doses of roscovitine as mentioned above. Twenty thousand nucleated marrow cells from these mice were plated in MethoCult M3434 and scored for CFU-GM, BFU-E and CFU-GEMM on day 12.

3.8 WESTERN BLOT

Immunoblotting was used to assess the activity of roscovitine in the brain tissues of the rats. The protein expression levels for CDK5-P35, ERK1, 2 and B-actin were determined in different brain regions for different time points until 48hr post administration (details in study II)

Immunoblotting analysis was done on supernatant obtained from homogenized brain tissues from treated and control animals. Equal amounts of proteins from these samples were separated by gel electrophoresis (SDS-PAGE) 10%. Proteins were then transferred to nitrocellulose membranes (Amersham Pharmacia Biotech) over night at +4 °C. The blots were blocked for 1 hr at room temperature in blocking buffer (TBS-T containing 7% BSA). Incubation with primary anti- Cdk5-p35 and pErk1/2 antibodies (1:1000 in wash blot with 5% BSA) was performed over night at room temperature. Following three washes with TBS-T for 10 min, the blots were incubated for 2 hr with horse raddish peroxidase-conjugated secondary antibodies (1:2000) at room temperature, washed and visualized using ECL (Amersham Pharmacia Biotech). Optical density of the bands was quantified with scion image (Scion Corporation, USA). The immunoblots were stripped using stripping buffer (Tris-HCl, pH 6.7, 2% SDS, mercaptoethanol) at +50 °C for 30 min, and then re-blotted with the antibodies of interest.

3.9 PHARMACOKINETICS ANALYSIS

Parameters including distribution volume of the central compartment, elimination rate constant, plasma maximum concentration (C_{max}) and micro constants were estimated. Clearance (Cl) and distribution volume at the steady state (V_{ss}) were calculated from the primary parameters. The plasma concentration versus time curves (AUC) were calculated from the model derived parameters and the elimination half-lives ($T_{1/2}$) were calculated from the slope of the terminal phase of elimination. Bone marrow data were derived after adjustment of concentrations to 10^9 cells (= approx. 1g of tissue). The pharmacokinetic modeling was performed using WinNonlin version 5.2.

Oral bioavailability (F) defined as the fraction of the oral administered dose of CR8 that reaches the systemic circulation. It was calculated according to the following

$$\text{formula: } F = \frac{[AUC]_{po} \times \text{Dose}_{iv}}{[AUC]_{iv} \times \text{Dose}_{po}}$$

3.10 *IN VITRO* METABOLISM OF ROSCOVITINE

Mice microsomal preparations

Male BDF1 mice were killed at either ZT3 or ZT19 and livers were weighted and snap frozen in liquid nitrogen. Microsomes were prepared by from the liver tissues by subcellular fractionation as described elsewhere [115, 116]. Briefly, pieces from liver tissues were homogenized by Potter-Elvehjem homogeniser in 2-4 times volume of potassium phosphate buffer (10 mM sodium/potassium phosphate/1.14% KCl, pH 7.4) and centrifuged at 10000g for 10 min followed by ultracentrifugation at 105000g for 70 minutes. All work was carried out at +4°C. Microsomal pellets were re suspended in 50mM potassium phosphate buffer (0.4 ml/liver) and stored at -80°C. Protein determination was carried out by a modified Lowry method [117] and bovine serum albumin was used as standard.

In vitro assay of microsomal metabolism of roscovitine

Different concentrations of roscovitine (0.5-10 μ Mol) were incubated at 37°C with the microsomal preparations (0.5 and 1mg/ml) in final volume of 0.5ml. Incubation was carried out for 0, 3, 5, 10, 20, 30, 45 and 60 minutes.

Reaction was terminated with the addition of 0.5 ml ice cold acetonitrile followed by vortex and centrifugation at 10000 rpm for 15 minutes to repel the proteins. 50 μ l of the supernatant were analyzed by HPLC as mentioned above. Rate of reaction was calculated from the disappearance of roscovitine. Data were plotted in logarithmic scale followed by linear regression and the reaction coefficient (k) was calculated as the slope of the regression line. *In vitro* intrinsic clearance (CL_{int}) values were calculated from initial rate of roscovitine disappearance and scaled up to the *in vivo* CL_{int} value by normalization to microsomal protein content, liver weight and body weight. Microsomal preparations from 3 mice were used for ZT 3 and other 3 for ZT 19.

3.11 STATISTICAL ANALYSIS

The results are presented as mean \pm S.D.

In study I, III, IV and V statistical analysis was performed using non-parametric Kruskal–Wallis and Mann–Whitney test, whenever appropriate. In study II Statistical evaluation was performed using a one-way ANOVA followed by Fisher's PLSD. P-value of less than 0.05 was considered as the level of significance.

4. RESULTS

4.1 PRECLINICAL PHARMACOKINETIC AND PHARMACODYNAMIC STUDIES OF ROSCOVITINE

4.1.1 PK and PD of roscovitine in the bone marrow in mouse

The present study was designed to investigate the clonogenic capacity of the bone marrow after exposure to roscovitine *in vitro* and *in vivo*.

4.1.1.1 Effect of roscovitine on the bone marrow cells *in vitro*

Incubation with roscovitine for 4 hr decreased the viability of bone marrow cells in a concentration-dependent manner. Roscovitine at 250 μM decreased the viability to 70% compared to controls ($p= 0.015$).

The clonogenic capacity of bone marrow cells to form CFU-GM, BFU-E and CFU-GEMM colonies after exposure to roscovitine was investigated in suspension cultures. Clonogenic capacity of the bone marrow decreased also in dose- and time-dependent manner. BFU-E were more sensitive than CFU-GM. BFU-E were completely blocked after 12 and 24 hr incubation with both 50 and 100 μM of roscovitine. Interestingly, short term incubation with roscovitine (250 μM) or DMSO for 4 hr did not affect the colony formation of any of the progenitors. However, a decrease in the colony formation in controls after 12 and 24 hr was observed which most probably is due to lack of the growth factors in the media.

Roscovitine induced suppression of colony formation in a concentration- and cell type- dependent manner in semi solid media containing growth factors supporting colony formation. CFU-GEMM were most sensitive and were completely blocked at 25 μM concentration, followed by BFU-E which were also significantly inhibited at 50 μM while CFU-GM were least sensitive and were inhibited at 100 μM only (Figure 5).

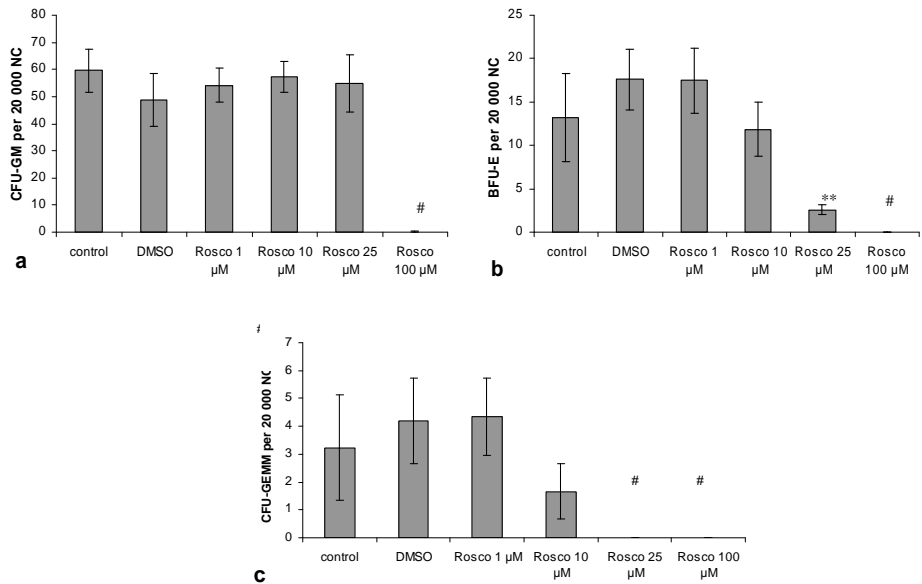


Figure 5. Effect of roscovitine on hematopoietic progenitors *in vitro*.

Twenty thousand of nucleated bone marrow cells were cultured in semi solid media (MethoCult M3434) with roscovitine at final concentrations of 1, 10, 25 or 100 μM or DMSO (control for solvent toxicity). CFU-GM (a), BFU-E (b) and CFU-GEMM were counted at day 12. Results are expressed as mean \pm SD from 5 mice. (** $p < 0.01$; # no colony were detected, thus significance could not be evaluated).

4.1.1.2 Effect of roscovitine on the bone marrow cells *in vivo*

After single dose of roscovitine up till 250 mg/kg, neither the number of nucleated cells nor the clonogenic capacity of the bone marrow was different compared to control mice. However, when roscovitine was administered for 4 days, transient inhibition of the BFU-E colonies occurred 1 day after of the last dose of roscovitine. Colony formation capacity of bone marrow was recovered 5 days after the last dose of roscovitine (Figure 6).

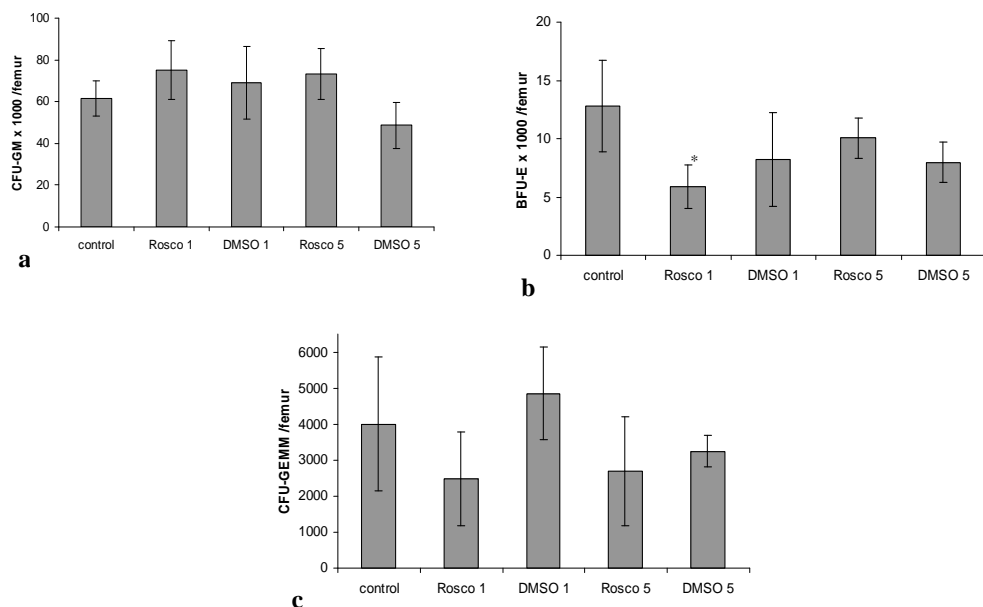


Figure 6. Effect of roscovitine on hematopoietic progenitors *in vivo*. Mice were treated with roscovitine (350 mg/kg) divided into two daily doses for 4 days. Mice treated with DMSO and untreated animals served as controls. Bone marrow was examined 1 and 5 days after the last dose of roscovitine. CFU-GM (a), BFU-E (b) and CFU-GEMM (c) were counted on day 12. Each group consisted of 5 mice, control group of 8 mice. Results are expressed as mean \pm SD.

4.1.1.3 Exposure time affects roscovitine-induced inhibition of hematopoietic progenitors

Longer incubation time using lower roscovitine concentration resulted in higher inhibition of colony formation compared to shorter incubation time with higher concentration, although both concentration and time combinations gave the same AUC (Figure 7).

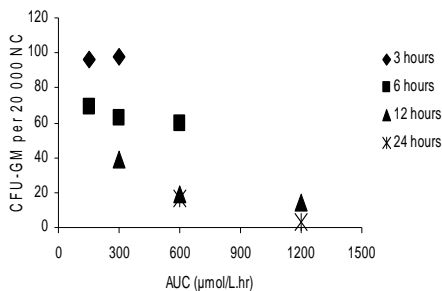


Figure 7. The influence of time on the effect of roscovitine on hematopoietic progenitors *in vitro*. Cells were incubated with roscovitine for 3, 6, 12 and 24 hr. Area under the concentration– time curve (*AUC*) has been estimated by trapezoidal rule.

4.1.1.4 Roscovitine pharmacokinetics and biodistribution to the bone marrow

Figure 8 shows the concentration-time curve of roscovitine in mouse plasma after single i.p. administration of 50 mg/kg. As presented in Table 1, only a small fraction of roscovitine (about 1.5%) compared to plasma reached the bone marrow.

Table 1 Plasma and bone marrow pharmacokinetic parameters following i.p. administration of roscovitine (50 mg/kg).

	<i>AUC</i> _{trapez}	<i>AUC</i> _{inf}	<i>C</i> _{max}	Cl	<i>V</i> _d	<i>T</i> _{1/2}
	µmol/L . hr	µmol/L .hr	µmol/L	L/hr	L	hr
Plasma	282.5	275.8	202	0.05	0.015	0.82
BM	4.1	4.6	4.9	0.62	0.54	0.61

(*BM*) Bone marrow, (*AUC*) area under the concentration–time curve, (*AUC*_{trapez}) *AUC* estimated using trapezoidal rule, (*AUC*_{inf}) *AUC* derived using Winnonlin analysis, (*C*_{max}) estimated maximum concentrations, (Cl) clearance, (*V*_d) apparent volume of distribution, (*T*_{1/2}) half-life

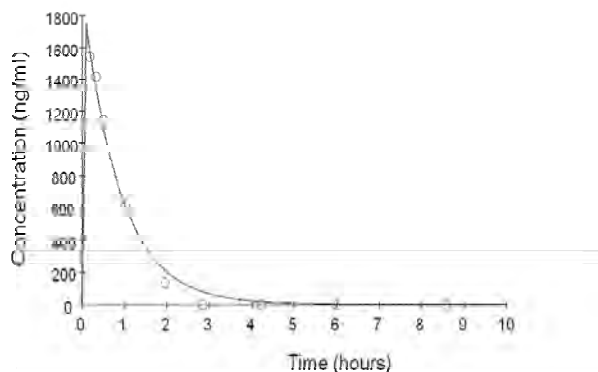


Figure 8. Area under the concentration–time curve in plasma after an i.p. dose of roscovitine (50 mg/kg).

4.1.2 Age-dependent kinetics and dynamics of roscovitine in rat brain

Study II aimed to explore the effect of age on the pharmacokinetics of roscovitine and to investigate the effect of roscovitine on two neuronal targets; Cdk5 and Erk1/2 in different brain regions.

4.1.2.1 Roscovitine pharmacokinetics and biodistribution into the brain in rats

Table 2 presents the pharmacokinetic parameters in plasma and different brain regions in 14-days old pups and adult rats, respectively, after single i.p. administration of 25 mg/kg roscovitine. The pharmacokinetics of roscovitine was fitted into 2-compartment open model with distribution half-lives of 0.6 hr in pups and 0.06 hr in adult rats. Significantly longer elimination half-life (7 hr) was observed in plasma and brain of the rat pups compared to 30 and 20 min found in plasma and brain in adult rats, respectively. This difference might explain the higher AUC in pups compared to adults.

No significant difference between roscovitine AUC in plasma and AUCs found in different brain regions in pups. On contrary, in adult rats the AUC of roscovitine in the brain was about 25 % of that found in plasma (Figure 9).

Table 2. Pharmacokinetic parameters in plasma and brain of adult and pups rats. Results are presented as mean \pm SD (n=3). (*AUC*) Area under the concentration–time curve; (*T α* , *T β*) distribution and elimination half-lives; (*C_{max}*) maximum concentration; (*V_{ss}*) volume of distribution; (*Cl*) clearance

PK parameters		Plasma	Frontal Cortex	Hippocampus	Cerebellum
AUC (hr.µg/ml)/ (hr.µg/g)	Pups	66.79 \pm 7.15	69.57 \pm 15	74.92 \pm 12	78.72 \pm 11.2
	Adults	3.01 \pm 0.21	0.71 \pm 0.14	0.58 \pm 0.03	0.62 \pm 0.06
T α (h)	Pups	0.50 \pm 0.09	0.48 \pm 0.19	0.43 \pm 0.1	0.59 \pm 0.14
	Adults	0.081 \pm 0.05	0.045 \pm 0.02	0.062 \pm 0.012	0.062 \pm 0.018
T β (h)	Pups	7.2 \pm 1.4	6.8 \pm 1.3	8.0 \pm 1.7	7.7 \pm 2.2
	Adults	0.54 \pm 0.26	0.35 \pm 0.13	0.36 \pm 0.15	0.42 \pm 0.18
C _{max} (µg/ml)/ (µg/g)	Pups	15.79 \pm 0.38	24.9 \pm 1.8	24.75 \pm 1.9	23.69 \pm 1.4
	Adults	17.71 \pm 4.42	4.47 \pm 0.70	4.64 \pm 0.81	3.81 \pm 1.22
V _{ss} (ml)	Pups	88 \pm 15.3	90 \pm 21	86 \pm 20	102 \pm 13
	Adults	650 \pm 223	1095 \pm 167	2056 \pm 219	1909 \pm 484
Cl (ml/h)	Pups	9.7 \pm 1.2	10.2 \pm 1.5	11.1 \pm 2	11.3 \pm 1.2
	Adults	1637 \pm 118	7262 \pm 1612	8737 \pm 452	8139 \pm 727

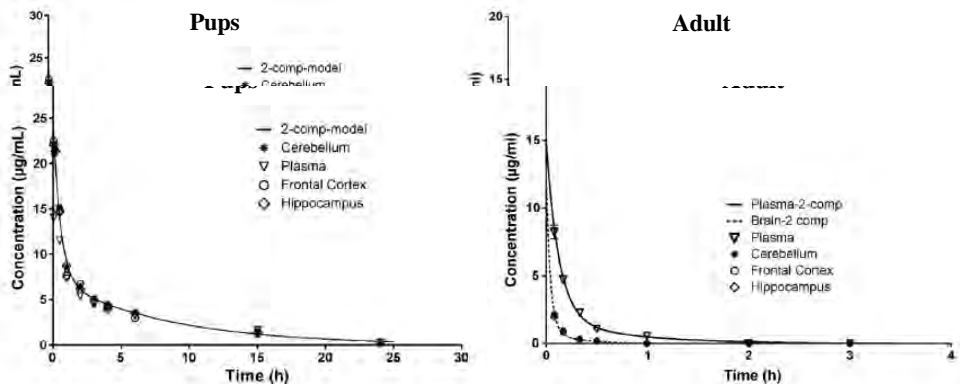


Figure 9: Concentration versus time curves of roscovitine after fitting to a two-compartment open model in the plasma and different brain regions in 14 days old rat pups and adult rats following single i.p. administration of 25 mg/kg. The solid line represents the theoretical model while (*) represents cerebellum, (∇) plasma, (o) frontal cortex, and (◆) hippocampus expressed as the mean of five animals at each time point.

The AUC of roscovitine was 22-fold higher in pups plasma and 100-fold higher in pups brain compared to that found in adult rats. The C_{max} was significantly ($p < 0.05$) higher ($>22 \mu\text{g/g}$) in pups brain compared to that found in plasma. However, the opposite was found in adult rats with the C_{max} 4-fold higher in plasma compared to that observed the brain ($17.7 \mu\text{g/ml}$ and about $4 \mu\text{g/g}$, respectively). The high concentrations of roscovitine found in the pups brain may indicate the free passage of roscovitine into the brain. No roscovitine metabolites were found in the brains of both adult and young rats.

4.1.2.2 Kinetics and effect of roscovitine on Cdk5 and Erk1/2 in different brain regions

In rat pups, roscovitine induced a transient and significant accumulation of p35 protein in all brain regions. This accumulation indicates the inhibition of the Cdk5 enzyme which phosphorylates the p35 protein, an essential step before its degradation. In frontal cortex, p35 was accumulated at 1–2 hr post-administration (140% of controls, Figure 10b, $p < 0.05$). In hippocampus and in cerebellum, a significant increase of p35 levels was observed at 2 hr post-administration (150% and 200%, respectively, Figure 10b). The levels of p35 were normalized at 6–15 hr (Figure 10a and b). No change in p35 levels was observed in the adult brain which probably is due to the low concentration and the rapid elimination half-life. Interestingly, the accumulation of p35 protein in the early time points after roscovitine administration was accompanied by increased levels of the phosphorylated (activated) form of Erk1/2. In frontal cortex and hippocampus, a transient activation of Erk1/2 was observed at 1 and 2 hr after injection (Figure 10a and b). In cerebellum, roscovitine induced a significant increase of pErk1/2 levels at 2 hr, followed by a significant decrease at 6 hr after administration (Figure 10b). At later time points, pErk1/2 levels were similar to controls, in all brain regions (Figure 10).

All together, roscovitine was presented in the brain of rat pups in sufficient amounts to inhibit the Cdk5 efficiently and that inhibition led to the increased phosphorylation of Erk1/2. The kinetics of roscovitine activity was short and rather similar in all brain regions.

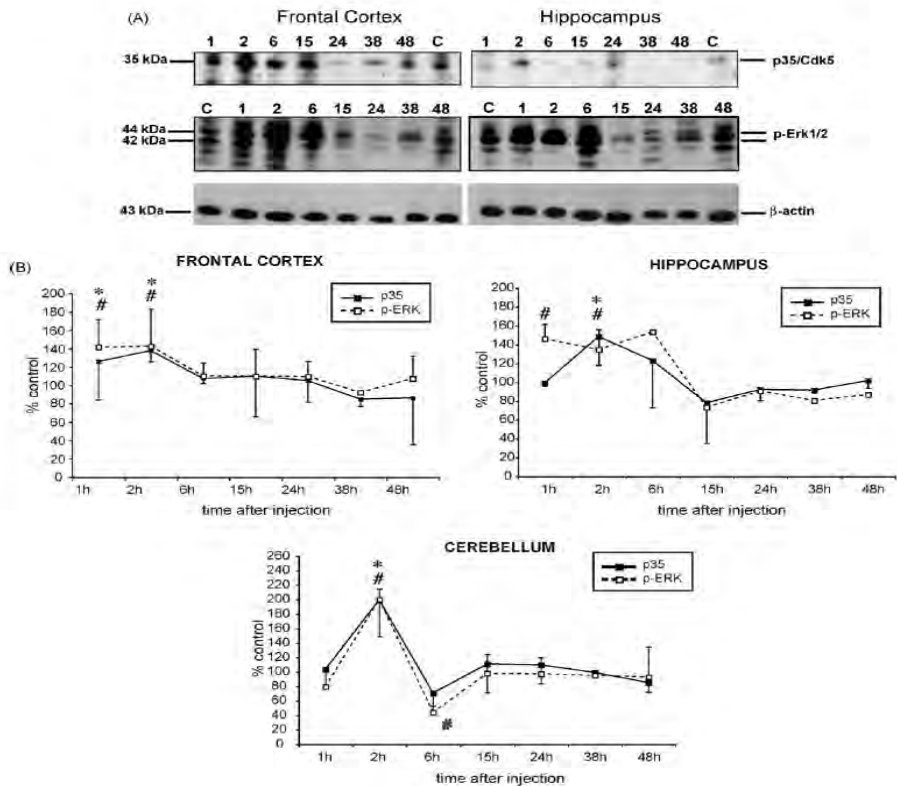


Figure 10. Effect of roscovitine on Cdk5-p35 and pErk in different brain parts of rat pups 14 days old after single i.p. injection of 25 mg/kg.

Pups were killed at different time points after injection, brains dissected, homogenized, and immunoblotted for active Cdk5-p35 and phosphorylated Erk1/2. The loading control was carried out using beta-actin. The bands were quantified using Scion image software.

(a) Immunoblotting of p35 and pErk1/2 in the frontal cortex and cerebellum. Animals were killed at the indicated time points after injection of roscovitine: C = animal injected with vehicle, used as control. (b) Densitometric analysis of the Western blotting bands for both p35 and pErk1/2 in the frontal cortex, hippocampus and cerebellum until 48 hr after single i.p. injection of roscovitine. Data are presented as mean \pm SD of values expressed as percentage of control animals (*, $p < 0.05$ for analysis of p35 data; #, $p < 0.05$ for analysis of p-ERK data; ANOVA followed by Fisher's PLSD post-hoc test).

4.1.3 Circadian rhythm-pharmacokinetics and metabolism of roscovitine

In the present study, we aimed to explore the effect of circadian rhythm on the pharmacokinetics, biodistribution and metabolism of the roscovitine. Roscovitine (300 mg/kg) was administered orally to male BDF1 mice either during their rest time (ZT3) or active time (ZT19).

4.1.3.1 Chronopharmacokinetics of roscovitine

The differences between ZT3 and ZT19 in the pharmacokinetic parameters of roscovitine are shown in Table 3. Significant ($p=0.04$) increase in the elimination half-life at ZT3 (4.6 hr) compared to ZT19 (1.93 hr). This led to a significant ($p=0.03$) higher exposure at ZT3 (AUC of 105 $\mu\text{g}\cdot\text{hr}/\text{ml}$) compared to that observed at ZT19 (AUC of 76 $\mu\text{g}\cdot\text{hr}/\text{ml}$). Volume of distribution at ZT19 was about one half of that at ZT3 ($p=0.04$) and clearance was faster at ZT19 by 38% ($p=0.048$). Maximum concentration (C_{max}) was significantly ($p=0.018$) higher (by 35%) at ZT19 compared to ZT3. A trend ($p=0.06$) was observed showing faster absorption half-life at ZT19 compared to ZT3. This might indicate a delay in the transit of roscovitine in the portal circulation.

Table 3. The pharmacokinetic parameters of roscovitine after single oral administration of 300 mg/kg at ZT3 or ZT19 to BDF1 male mice.

PK parameters		ZT3	ZT19	P-value
AUC	(h. $\mu\text{g}/\text{ml}$)	105.8 \pm 13.9	76.7 \pm 6.3	0.03
$T_{1/2\ \alpha}$	(h)	0.31 \pm 0.08	0.14 \pm 0.08	0.06
$T_{1/2\ \beta}$	(h)	4.6 \pm 1.09	1.93 \pm 0.34	0.02
C_{max}	($\mu\text{g}/\text{ml}$)	14.5 \pm 1.8	19.9 \pm 0.4	0.02
V_d	(ml)	370 \pm 70	210 \pm 30	0.048
CL	(ml/h)	60 \pm 10	80 \pm 10	0.044

Results are presented as a mean \pm SD of three animals for each time point. (AUC) Area under the concentration–time curve; ($T_{1/2\ \alpha}$) distribution half-life; ($T_{1/2\ \beta}$) elimination half-life; (C_{max}) maximum reached concentration; (V_d) volume of distribution at steady state; (CL) clearance.

4.1.3.2 Chronobiodistribution of roscovitine

The organs to plasma ratios of roscovitine exposure expressed as AUC adjusted per gram wet tissue are presented in Table 4. Significant increase in the organ to plasma ratio of roscovitine was found after administration of roscovitine at ZT3 in the adipose tissue (188%), kidney (180%), testis (133%) and lungs (112%). However, the distribution to the liver was significantly ($p=0.01$) higher at ZT19 (120%). No differences in brain or intestine were observed.

Table 4: The exposure to roscovitine expressed as AUC in plasma (hr.µg/ml) and different organs (hr.µg/g). Roscovitine was administered as single oral dose (300 mg/kg) at either Zeitgeber time ZT3 or ZT19 (n=3).

Organ	ZT3	ZT19	P -value*
Plasma	105.8 ± 13.9	76.7 ± 6.3	0.03
Liver	285.9 ± 7.2	342.3 ± 23.0	0.01
Kidney	261.7 ± 56.5	145.2 ± 17.3	0.02
Adipose	313.8 ± 48.7	166.6 ± 43.6	<0.001
Testis	49.3 ± 2.1	37.0 ± 3.5	0.003
Lung	161.2 ± 8.2	143.0 ± 9.5	0.05
Intestine	2421 ± 626	2484 ± 629	0.40
Brain	16.6 ± 2.3	12.9 ± 1.9	0.10

4.1.3.3 The metabolic ratio of roscovitine was higher at ZT3 compared to ZT19

The metabolic ratio was calculated as the ratio of AUC of the carboxylic metabolite of roscovitine (M1) / AUC of roscovitine. The systemic metabolic ratio of roscovitine was found to be about 3.8 at ZT19 while it is only about 3.08 at ZT3. The metabolic ratio at ZT19 was 23% higher ($p<0.05$) compared to that found at ZT3.

4.1.3.4 Intrinsic clearance of roscovitine (CL_{int}) was higher at ZT3 compared to ZT19

In order to investigate the possible difference in metabolism of roscovitine due to circadian rhythm, roscovitine was incubated *in vitro* with liver microsomes from mice killed at either ZT3 or ZT19. Three mice were used for each time point. Figure 11 shows roscovitine concentration-time curves after *in vitro* microsomal incubation of 2.5 μM roscovitine with liver microsomes.

There is a faster and complete metabolism of roscovitine after approximately 45 min at ZT19. However, at ZT3 the disappearance of roscovitine was slower and the drug was not completely eliminated until 60 minutes.

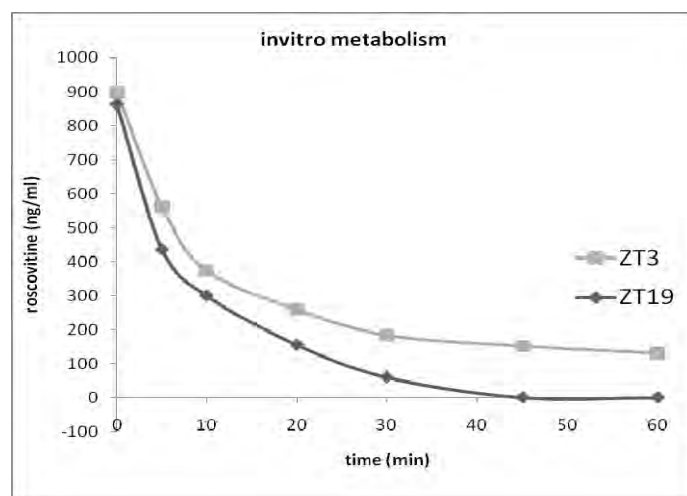


Figure 11. Roscovitine time-concentration curve after incubation of 2.5 μM roscovitine with microsomal preparations (1 mg/ml) from liver tissues taken either at ZT3 or ZT19.

Calculation of the *in vivo* intrinsic clearance confirmed higher rate of metabolism and higher CL_{int} in mice at ZT19 ($CL_{int}=70 \mu\text{l}/\text{min}/\text{mg}$ protein) compared to that obtained in mice at ZT3 ($CL_{int}=43.3 \mu\text{l}/\text{min}/\text{mg}$ protein). The difference was significant with p value of 0.007 (Table 5).

The amount of microsomal proteins per gram of liver tissue showed no significant difference between microsomes prepared from the livers taken at ZT19 and ZT3. That might indicate a faster metabolic reaction and higher enzyme affinity rather than a significant difference in the CYP450 amount.

Table 5. Roscovitine *in vivo* intrinsic clearance values (CL_{int}) after *in vitro* incubation of roscovitine with microsomal preparations (1 mg/ml) from 3 BDF1 mice killed at ZT3 and ZT19.

CL_{int} ($\mu\text{l}/\text{min}/\text{mg}$ protein)				Mean	SD	P-value	ZT19/ZT3
ZT19	68,87	78,00	62,50	69,79	7,79	0,007	1,61
ZT3	39,66	42,06	48,26	43,33	4,44		

The CL_{int} value was calculated from initial rate of roscovitine disappearance and normalized to microsomal protein content, liver weight and body weight. Results were compared using 2 tailed unpaired t-test.

4.2 SECOND GENERATION ANALOGUES OF THE CYCLIN DEPENDENT KINASE INHIBITORS

4.2.1 N-&-N, a new class of kinase inhibitors derived from roscovitine

4.2.1.1 Synthesis of two bioisoster analogues of roscovitine

Two compounds closely related to roscovitine were synthesized, N-&-N1 and N-&-N2. The shift of the nitrogen from position 9 in the purine ring of roscovitine to position 5 (N-&-N1) or position 4 (N-&-N2) equivalents has led to significant increase in the potency and efficacy compared to the parent compound (Figure 12).

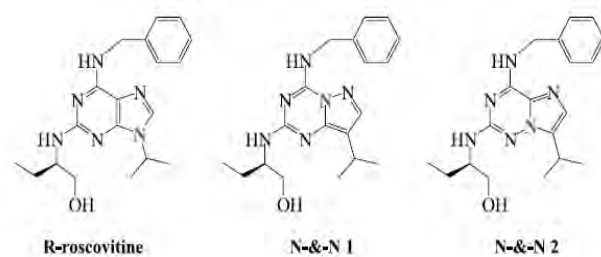


Figure 12: structure of (R)-roscovitine, N-&-N1, and N-&-N2.

4.2.1.2 Kinase inhibition by the two roscovitine analogues

(R)-roscovitine, N-&-N1, and N-&-N2 were tested on the major roscovitine targets (Cdk1/cyclin B, Cdk2/cyclin A, Cdk2/cyclin E, Cdk5/p25, Cdk7/ cyclin H,

Cdk9/cyclin T, CK1 γ /q, Dyrk1A, and Erk2) and the GSK-3 α/β (Table 6). N-&-N1 was found to be significantly more active on all Cdks compared to either (R)-roscovitine or N-&-N2. N-&-N1 was three to five times more active on CK1 and GSK-3 α/h compared to (R)-roscovitine but both were roughly equipotent on Erk2.

Table 6: Effects of the three molecules on ten protein kinase targets. Compounds were tested at various concentrations in the kinase assays as described in Materials and Methods. IC50 values were calculated from the dose response curves and are reported in $\mu\text{mol/L}$.

Kinase	(R)-roscovitine	N-&-N1	N-&-N2
CDK1/cyclin B	0.33	0.073	0.40
CDK2/cyclin A	0.22	0.04	0.22
CDK2/cyclin E	0.15	0.026	0.16
CDK5/p25	0.27	0.07	0.32
CDK7/cyclin H	0.80	0.5	0.60
CDK9/cyclin T	0.23	0.043	0.20
CK1	4.00	1.20	1.20
DYRK1A	3.00	1.30	2.00
Erk2	11.0	18.0	10.0
GSK-3 α/β	60.0	11.0	30.0

4.2.1.3 *N-&-N1 induces apoptotic cell death*

The effect of the two compounds was compared with roscovitine on their activity on the SH-SY5Y neuroblastoma cell lines. Dose-response curves showed that (R)-roscovitine and N-&-N2 displayed similar activities while N-&-N1 was consistently more potent in terms of concentration required to reduce cell survival (MTS reduction; Figure 13A and B) or in terms of cell death (lactate dehydrogenase release; Figure 13C). The three compounds induced a strong reduction of retinoblastoma protein phosphorylation and a dramatic down-regulation of the Mcl-1 survival factor (Figure 13D). Both biochemical events were induced with the lowest concentrations of N-&-N1.

After that we tested (R)-roscovitine, N-&-N1, and N-&-N2 on seven human cell lines (Table 7). With the exception of human fibroblasts, all cell lines were more sensitive to N-&-N1 (average IC₅₀ = 5.2 μmol/L) than to (R)-roscovitine (average IC₅₀ = 28.3 μmol/L) or N-&-N2 (average IC₅₀ = 25.0 μmol/L).

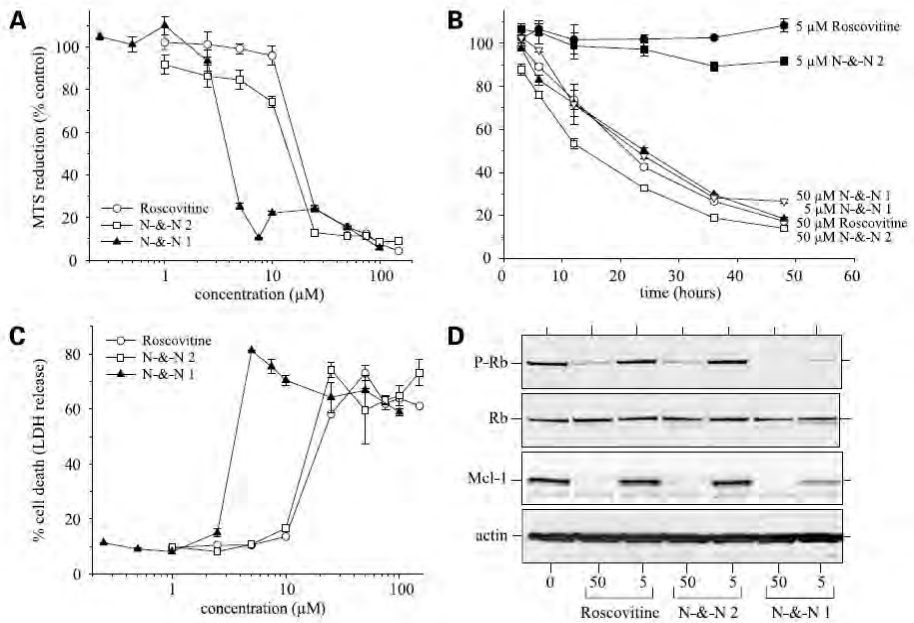


Figure 13. Effects of (R)-roscovitine, N-&-N1, and N-&-N2 on SH-SY5Y cells. (A) SH-SY5Y cells were exposed for 24 hr to increasing concentrations of the three compounds. Cell survival was estimated by the MTS reduction assay and is expressed in percentage of survival in untreated cells. Average \pm SE of at least four independent experiments with three independent measurements per experiment. (B) time-course experiment: SH-SY5Y cells were treated with 5 or 50 μmol/L of each compound for 3, 6, 12, 24, 36, or 48 hr. Cell survival was assessed by the MTS assay. Points mean of two independent experiments with at least three independent measurements per experiment; bars, SE. (C) an experiment similar to that presented in (A) was done, but lactate dehydrogenase release was assayed 24 hr after the addition of the compounds. Average \pm SE of two independent experiments with three independent measurements per experiment. (D) SH-SY5Y cells were exposed to 5 or 50 μmol/L of each compound for 24 hr and proteins were resolved by SDS-PAGE followed by Western blotting with antibodies directed against phospho-Rb, Rb, Mcl-1, and actin.

Table 7. Effects of the three molecules on the survival of various cell lines. (R)-roscovitine and its two analogues were tested at various concentrations for their effects on seven different cell lines: cell survival was estimated 48 hr after the addition of each compound using the MTS reduction assay. IC50 values were calculated from the dose response curves and are reported in $\mu\text{mol/L}$. Average \pm SE of two independent measurements done in triplicates.

cell line	(R)-roscovitine	N-&-N1	N-&-N2
HCT116 (colon)	20.8	2.4	19.4
MDA-MB-231 (breast)	29.5	8.0	28.0
Huh7 (hepatoma)	23.8	3.8	26.0
F1 (hepatoma)	31.0	6.9	29.3
SH-SY5Y (neuroblastoma)	17.2	2.6	17.3
HEK 293 (embryonic kidney)	47.7	7.6	30.2
average 6 cell lines	28.3	5.2	25.0
human foreskin fibroblasts	> 30.0	> 30.0	> 30.0

4.2.1.4 Quantitative analysis of N-&-N1

To investigate the pharmacokinetics of N-&-N1, HPLC-UV method was developed to detect the drug in plasma and other biological samples. Sample preparation was done by simple protein precipitation using methanol (1:2 v:v). The UV absorbance scan showed good absorption in the UV wavelength range (210 - 250 nm), with highest absorption at 215-220 nm.

The chromatographic conditions were reported in details in the materials and methods.

4.2.1.5 Validation of the analytical method

The analytical method was validated and was shown to provide enough selectivity, sensitivity, and stability for pharmacokinetic studies according to the bioanalytical guidelines mentioned by Shah et al [112].

Chromatography and selectivity

Selectivity was confirmed by absence of interference in the entire range of the largest peak. The retention time of N-&-N 1 was 21 ± 1 min (Figure 14).

Linearity and limit of quantification

The calibration curve was linear within the range of 100 ng/mL to 5 µg/mL with correlation coefficient (r^2) ≥ 0.9987 . The between-run variation in the curve slope was 0.443 ± 0.017 . The lower limit of quantification (LLOQ) for N-&-N 1 was 100 ng/mL in human plasma. The precision and accuracy at LLOQ were 11.7 and 5.5 %, respectively.

Accuracy and precision

The between-run and within-run precision and accuracy are summarized in Table 8. The precision and accuracy between and within batch were always below 14% from the nominal values in all cases. Precision and accuracy fulfilled the guiding principles for validation of bioanalytical methods, i.e. < 15% for QCs both between batches and within batches and < 20% for LLOQ.

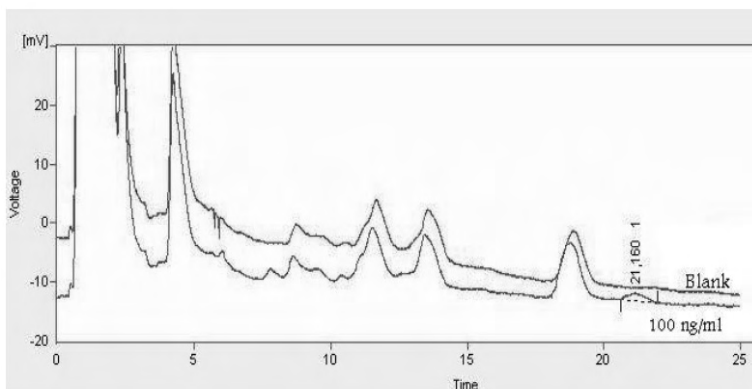


Figure 14. HPLC sample chromatograms of blank and N-&-N 1 at 100 ng/mL (LLOQ).

Recovery

The absolute recovery of N-&-N 1 in plasma was $80 \pm 2.0\%$ at the concentration of 750 ng/mL, while the relative recovery of the drug at the same concentration in plasma compared to methanol was $93 \pm 1.2\%$. The recovery from plasma was high with low limit of quantification as less as 100 ng/mL.

Stability

The drug was stable after 24 hr at room temperature. No significant decrease in the concentration of the low and middle QC samples was detected.

Table 8. Precision and accuracy of the N-&-N 1 analysis.

Concentration (ng/ml)	Precision (%)			Accuracy (%)		
<i>Between batch</i>						
100 (LLOQ)	10.3			-6		
300 (QC1)	6.5			5.4		
750 (QC2)	2.8			6.4		
4000 (QC3)	1.7			5.6		
<i>Within batch</i>	<i>Batch1</i>	<i>Batch2</i>	<i>Batch3</i>	<i>Batch1</i>	<i>Batch2</i>	<i>Batch3</i>
100 (LLOQ)	10.9	12.2	8.0	-4.4	-13.4	0.2
300 (QC1)	5.2	11.8	7.8	-3.4	7	3.4
750 (QC2)	4.0	6.7	3.2	7.1	2.2	7.1
4000 (QC3)	2.3	2.1	2.2	3.2	12.3	3.6

4.2.1.6 Pharmacokinetics of N-&-N1 in mouse

We investigated the PK of N-&-N1 in female Balb/c mice after i.p. administration of a single dose of 25 mg/kg. The PK parameters are listed in table 9. Variability of the results was low between the two mice experiments. The PK was found to fit a two-compartment open model Figure 15. The elimination half-life was biphasic with rapid distribution (9 min) and an elimination half-life of 1 hr.

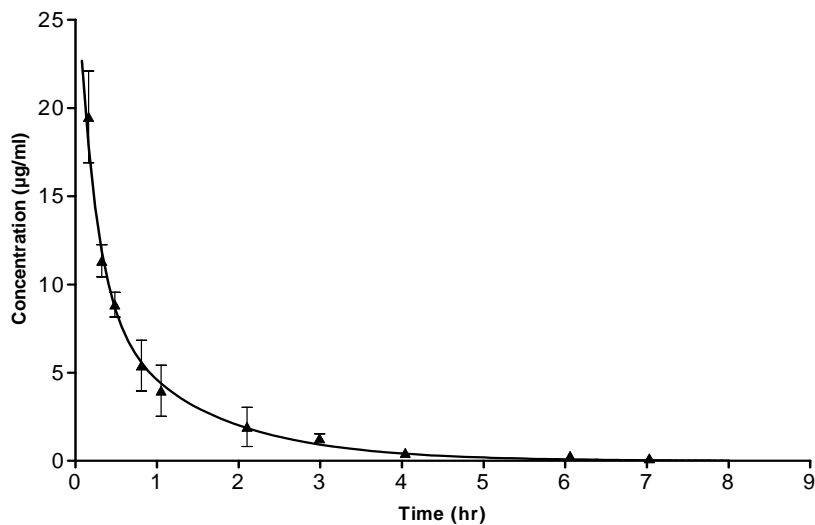


Figure 15. Pharmacokinetics of N-&N1 in mice.

The pharmacokinetics of N-&N1 were fitted a two-compartment open model. The elimination half-life was biphasic with rapid distribution and an elimination half-life of 1 hr. Area under plasma concentration curve. Solid line, two-compartment model; filled circles, experimental time points \pm SD. Each time point includes two animals

Table (9) PK parameters of N-&N1 in female Balb/c mice after single administration of 25mg/kg i.p.

Parameter	Mean	S.D.	C.V. (%)
AUC ($\mu\text{g/ml min}$)	18.5	1.9	10.3
$T_{1/2}$ -alfa (min)	8.9 min	0.095	0.11
$T_{1/2}$ -beta (min)	58.14	4.96	8.5
Cl (ml/min)	27.335	2.819	10.3
Vd. (ml)	0.028	0.0023	8.3
Cmax ($\mu\text{g/ml}$)	36.274	6.758	18.6

4.2.2 Pharmacokinetics and biodistribution of CR8

CR8 was introduced as a second generation inhibitor of cyclin-dependent kinases (Cdks) derived from roscovitine. CR8 was shown to be 50-100-fold more potent than roscovitine in inducing apoptosis in different tumor cell lines. In the present investigation we established an analytical method to quantify CR8 in biological samples and we studied its bioavailability, biodistribution and pharmacokinetics in mice.

4.2.2.1 *Quantitative analysis of CR8*

To investigate the pharmacokinetics of CR8; a precise and accurate analytical method using HPLC-UV was developed to detect the drug in plasma and other biological samples.

Sample preparation was done by simple protein precipitation using methanol. UV-scan showed good absorption wavelength range 210 - 310 nm. 305 nm was selected as the best measurement wavelength to ensure good selectivity and good sensitivity.

4.2.2.2 *Validation of the analytical method*

The analytical method was validated and was shown to provide enough selectivity, sensitivity, and stability for pharmacokinetic studies according to the bioanalytical guidelines.

Chromatograms and selectivity

The CR8 retention time was around 5.5 ± 0.3 min. Selectivity was confirmed by the absence of significant interfering peaks from endogenous compounds in the blank plasma at this retention time. Also, no interference was found from metabolites in the mice plasma and tissue samples compared to control samples (Figure 16).

Linearity and limit of quantification

The calibration curve was linear within the range of 0.1 $\mu\text{g/mL}$ to 10 $\mu\text{g/mL}$ with a correlation coefficient (r^2) ≥ 0.9987 . The lower limit of quantification (LLOQ) for CR8 was 100 ng/mL in human plasma. The precision and accuracy at LLOQ were 3.7 and -13.3%, respectively.

Accuracy and precision

The between-run and within-run precision and accuracy results are provided in Table 10. The precision and accuracy between and within batch were always below 13% from the nominal values in all cases. Precision and accuracy fulfilled the standard guiding principles for validation of bioanalytical methods, i.e. < 15% for QCs both between batches and within batches and < 20% for LLOQ.

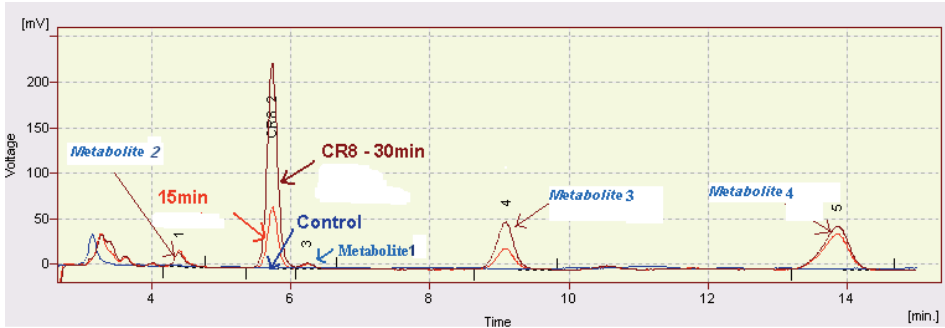


Figure 16. HPLC chromatograms of mice plasma samples from control mice and plasma taken after 15 min and 30 min from treated mice with CR8 as 100 mg/kg orally.

Table 10. Precision and accuracy of the CR8 analysis

Concentration (µg/ml)	Precision (%)			Accuracy (%)		
<i>Between batch</i>						
0.1 (LLOQ)	3.7			-13.3		
0.75 (QC1)	7.7			-2.0		
1.5 (QC2)	6.9			-3.8		
3.5 (QC3)	4.9			-4.4		
7.0 (QC4)	3.3			-5.3		
<i>Within batch</i>						
	<i>Batch1</i>	<i>Batch2</i>	<i>Batch3</i>	<i>Batch1</i>	<i>Batch2</i>	<i>Batch3</i>
0.1 (LLOQ)	4.2	3.4	4.8	-16	-15.4	-8.5
0.75 (QC1)	1.4	1.8	1.9	5.5	-12.9	-1.2
1.5 (QC2)	1.5	1.7	0.8	4.3	-6.7	3.0
3.5 (QC3)	0.2	0.6	1.1	-9.1	-9.9	-0.6
7.0 (QC4)	0.8	2	1.3	-3.5	-7.4	-4.1

Recovery

The absolute recovery of CR8 in plasma was 95 ± 5.0 % tested at the concentration of $1.5 \mu\text{g/mL}$, while the relative recovery of the drug at the same concentration in plasma compared to aqueous solution was 103 ± 1.2 %. The recovery from plasma was high, with low limit of quantification as less as the LLOQ.

Stability

The drug proved to be stable after 2 months at room temperature, $+4$ °C and -20 °C, with no significant decrease in the concentration of the QC samples (approximately 98 ± 3.5 %).

4.2.2.3 CR8 Metabolites

Four CR8 metabolites were successfully separated with good specificity and found to absorb UV at the same wavelength as CR8 (Figure 16). The first metabolite (M1) appeared at 6.1 ± 0.1 min., just after CR8, the second metabolite (M2) at 4.2 ± 0.2 min., the third metabolite (M3) at 9 min. and the fourth metabolite (M4) at about 14 min. The first metabolite (M1) was found to increase with time and accumulate with slow clearance compared to CR8 (Figure 17).

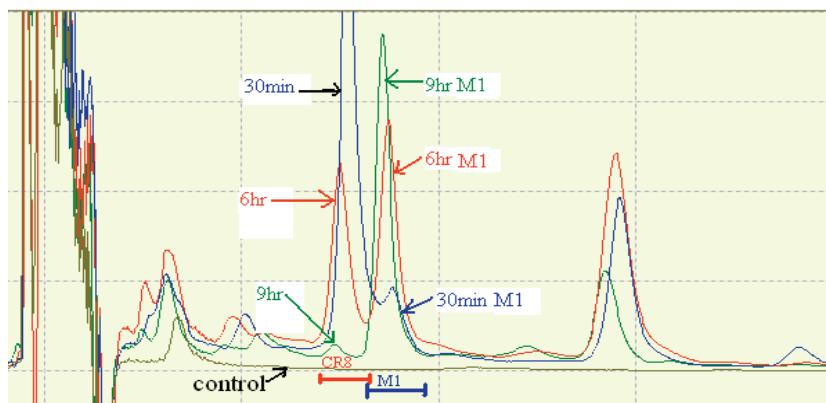


Figure 17. HPLC chromatograms of plasma of mice taken at 30min, 6hr and 9hr after CR8 administration as 50 mg/kg. One of CR8 metabolites called M1 shows accumulation with time.

4.2.2.4 Pharmacokinetics of CR8

The pharmacokinetics of CR8 was then investigated in mice and found to fit a two-compartment open model after oral and i.v. administration (Table 10) using Gauss-Newton criteria.

Absorption and distribution were rapid and the maximum concentrations were found at 30 min and most importantly the elimination half-life was estimated to be about 3 hours.

Exposure to concentrations much higher than the reported average IC50 value (0.7 μ M) [81] was found to last more than 8-10 hours (Figure 18). The oral bioavailability of CR8 was found to be essentially 100%.

Table 11. Pharmacokinetic parameters of CR8 following single oral administration of 100 mg/kg and i.v. bolus administration of 50 mg/kg.

PK parameters	Oral	i.v.
AUC (hr. μ g/ml)	96.3 \pm 10.5	43.4 \pm 3.3
T $\frac{1}{2}$ α (hr)	1.3 \pm 0.4	0.11 \pm 0.01
T $\frac{1}{2}$ β (hr)	3.1 \pm 0.4	2.95 \pm 0.11
C $_{\max}$ (μ g/ml)	34.3 \pm 1.9	163.9 \pm 0.3
Vd (ml)	21 \pm 3	44 \pm 4
Cl (ml/hr)	21 \pm 2	23 \pm 2
Bioavailability (F)	(96.43*50)/(43.35*100)*100 = 111%	

Results are presented as mean \pm SD (n=2). (AUC) Area under the concentration–time curve; (T α , T β) distribution and elimination half-lives; (C $_{\max}$) maximum concentration; (Vd) volume of distribution; (C) clearance.

Oral AUC of CR8

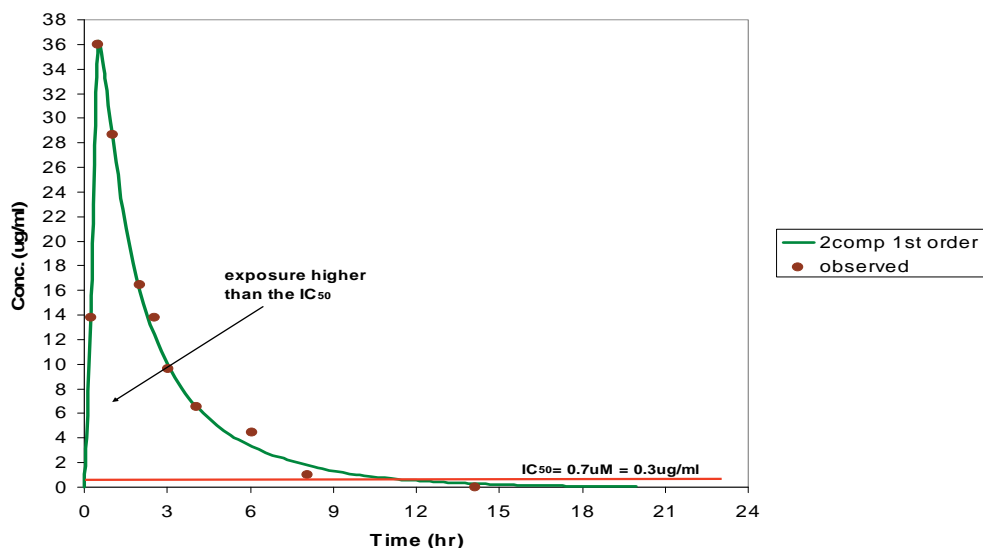


Figure 18. AUC of CR8 in plasma of Balb/c mice administered orally (50 mg/kg). The dashed area represents the systemic exposure to CR8 above the *in vitro* IC₅₀ reported in tumor cell lines.

4.2.2.5 Biodistribution of CR8

CR8 was widely distributed into all tissues and the time-concentration curves (AUC's) were fitted to one compartment model for all tissues (Table 11).

Higher exposure compared to that observed as systemic exposure in plasma was found in the liver (200%), adipose tissue (180%) and kidneys (150%). Lung and spleen showed a tissue/plasma ratio of 80% and 50%, respectively (Figure 19).

CR8 distribution to the bone marrow

Exposure to CR8 was about 30% in the bone marrow compared to that seen in plasma when the concentrations were normalized to tissue weight by grams (Figure 19). This exposure is higher for more than 6 hr than reported IC₅₀ in leukemic cell lines (data not shown).

CR8 distribution to the brain

CR8 was found to pass the BBB and the concentration in the brain was about 15% of that in plasma. Despite this low brain/plasma ratio, the concentration reached a value above the reported Cdk5/p25 and casein kinase 1 (CK1) inhibitory IC₅₀ values for more than 6 hours.

Table 12. Biodistribution of CR8 to different compartments following single oral administration of 100 mg/kg and i.v. bolus administration of 50 mg/kg.

	plasma	liver	adipose tissue	kidney	lung	spleen	BM	brain
AUC (hr.µg/ml)/ (hr.µg/g)	96.3	197.0	181.0	145	77	40	33.8	14
T _½ β (hr)	3.1	2.43	2.40	2.62	2.58	2.60	1.98	2.12
Cl _{max} (hr.µg/ml)/ (hr.µg/g)	34.3	52.4	48.7	36.0	19.3	27.7	10.6	4.1
Cl/F	21.0	10.2	11.1	13.8	26.2	20.0	29.5	146.0
Vd	21.0	35.8	38.2	52.2	96.7	74.5	84.5	447.5

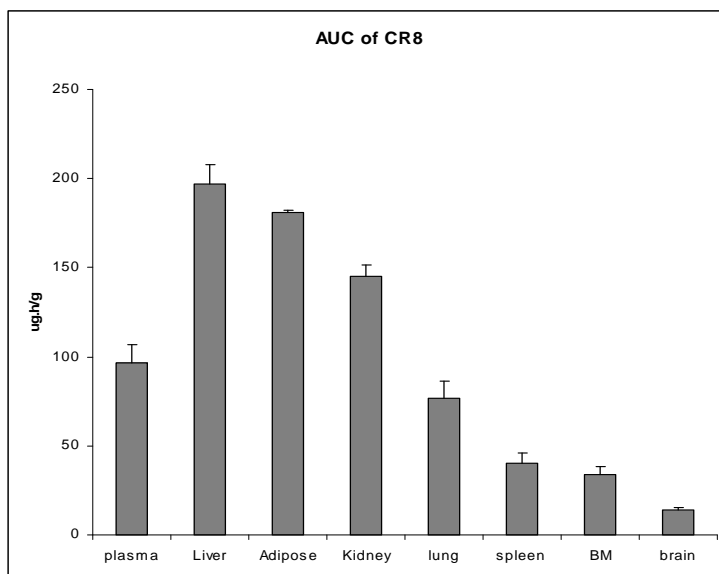


Figure 18. Tissue exposure to CR8 after oral administration of 100 mg/kg to female Balb/c mice. Plasma AUC units is hr.µg/ml.

5. DISCUSSION

Cyclin-dependent kinases (Cdks) are serine/threonine kinases that play key roles in the regulation of cell cycle progression and RNA transcription. Cdk over activity has been described in most types of cancer and is mediated by several genetic and epigenetic changes. Synthetic cyclin dependent kinase inhibitors (Cdk_i) are small molecular heterocyclic compounds which compete with ATP and inhibit the phosphorylation of the target substrates. Exposure of tumor cells to Cdk_i can lead to both cell cycle arrest and apoptosis.

The family of 2,6,9-trisubstituted purines are one of the first described Cdk inhibitors [118]. Among these purines the (R)-stereoisomer of roscovitine has now reached phase-II clinical trials for NSCLC and nasopharyngeal cancers and phase-I trials for glomerulonephritis. Several other preclinical studies are currently investigating the possible use of roscovitine in the treatment of neurodegenerative disorders such as Alzheimer's disease, viral infections (e.g. HIV and CMV), protozoal infections (e.g. leishmania and malaria) and inflammatory diseases (e.g. Lupus and GVHD). Roscovitine has rapid metabolism and short elimination half-life in rodents and man [53, 72, 74, 75]. The poor pharmacokinetic profile and the insufficient exposure to roscovitine in cancer patients may explain the modest success in the clinical trials [76]. Current research is focusing on overcoming pharmacokinetic barriers that hindered the clinical use of roscovitine, as well as development of novel classes of second generation analogues of roscovitine. Recent study on the pan-Cdk inhibitor flavopiridol has confirmed the importance of optimizing the schedule of dosing according to the PK/PD relationship. Significant difference in the clinical outcome and final response of refractory CLL patients was achieved by changing the dose schedule from 72 hr infusion to 30 minutes i.v. bolus followed by 4-hr-infusion [119].

In the present thesis, we aimed to explore different aspects of roscovitine pharmacokinetics and pharmacodynamics in order to improve the PK profile and to establish the PK/PD relationship which may help to design proper dosages schedules in the clinical trials. We have also developed new analytical methods and studied the PK profile of two second generation analogues of roscovitine. These data are crucial in the early development of these drugs.

5.1 MYELOSUPPRESSION

Myelosuppression is one of the most frequent complications and a dose limiting factor for the majority of conventional chemotherapeutic agents. In order to investigate the myelosuppressive potential of roscovitine we studied the effect of roscovitine on bone marrow progenitors *in vitro* and *in vivo*. Our results showed that the viability of bone marrow cells was significantly reduced at concentrations as high as 250 μ M while lower concentrations did not have significant effect. Our results were in agreement with the findings that roscovitine induced apoptosis of mature neutrophils [120], eosinophils [121] and proliferating T-cells [122] in a concentration and exposure-time dependent manner. Incubation of bone marrow cells with roscovitine in media supplemented with FBS was not used longer than 4 hours since the lack of relevant growth factors resulted in decreased clonogenic capacity of hematopoietic progenitors incubated with media/FBS for longer time. Interestingly the clonogenic capacity of the hematopoietic progenitors was not affected after 4 hours incubation with roscovitine in all concentrations studied. We speculated that the short incubation time with roscovitine might not be enough to allow the drug to exert its effect on the clonogenic capacity of bone marrow cells. That was also observed with malignant cell lines and the optimum exposure time for roscovitine to exert antitumor growth inhibition was between 8-16 hr [53]. Longer exposure of bone marrow cells to roscovitine was performed in the semisolid MethoCult media supplemented with recombinant growth factors required for the growth of the primary hematopoietic progenitors. Roscovitine decreased the colony formation of all the progenitors in cell type- and concentration-dependent manner. CFU-GEMM colonies were most sensitive, followed by BFU-E colonies and the least sensitive were CFU-GM colonies. This finding is in line with other studies showing the difference in sensitivity between erythroid colonies and granulocyte-macrophage colonies using other chemotherapeutic agents [123].

The myelosuppressive effect of roscovitine was studied *in vivo* in female Balb/c mice. Roscovitine was administered to the mice and bone marrow cells were cultured in the MethoCult media and assessed for clonogenic growth. Surprisingly, no myelosuppressive effect was detected after the administration of a single dose of roscovitine up to 250 mg/kg. Moreover, multiple

administrations of 175 mg/kg twice daily for 4 days did not induce significant myelosuppression except only a transient inhibition of the BFU-E detected one day after the last dose. The lack of activity of roscovitine on hematopoietic progenitors *in vivo* was not expected because of its proven inhibitory effect *in vitro* and the reported activity on different xenografts *in vivo* using the same or lower concentrations [45, 53, 68, 69]. In this study we found that the AUC of roscovitine in bone marrow was less than 1.5% of the plasma AUC and the elimination half-life of roscovitine was less than 1 hr. The short half-life and the low exposure might explain the absence of myelosuppression *in vivo*. The obtained results have pointed out two critical issues; firstly, what is the effect of exposure time to roscovitine on the hematopoietic progenitors? We found that roscovitine effect on the hematopoietic progenitors is exposure time-dependent. Given the same AUC, lower roscovitine concentration with longer incubation time results in higher inhibition of colony formation compared to higher concentration of roscovitine with shorter incubation time. This relation is different from other chemotherapeutic agents whose myelosuppressive effect has a linear relationship with the total AUC independent of the incubation time [124-126]. Secondly, what is the sensitivity of the hematopoietic progenitors *in vitro* to roscovitine in comparison to the sensitivity of the tumor cells? The hematopoietic progenitors were inhibited by roscovitine within the same exposure range as the tumor cells when comparing the inhibitory AUC reported for tumor cell lines [45, 53] with the inhibitory AUC of the hematopoietic progenitors found in our study.

No myelosuppression has been reported until now in the preclinical and clinical studies with roscovitine [73, 76], which is in agreement with our *in vivo* study, however in some special situation the myelosuppressive potential of roscovitine could be evident such as:

- 1- In combination with radiation therapy which increase distribution of some drugs to the bone marrow by increasing the permeability of blood-bone marrow barrier [127] or in combination with chemotherapy with myelosuppressive properties. Precautions should be taken in clinical trials.
- 2- In pediatric patients where age-dependent changes of roscovitine PK is most likely (e.g. longer elimination half-life). In such conditions higher exposure of

hematopoietic progenitors to roscovitine might occur which may increase toxicity risk [128].

5.2 AGE-DEPENDENT PHARMACOKINETICS

The determination of age-dependent pharmacokinetics is very important when the drug is clinically indicated in pediatric patients and/or when the drug has very narrow therapeutic window. This is important for scheduling the correct doses and to avoid toxicities. Roscovitine has been found to inhibit different solid and hematological tumor cell lines including ALL [129] which is frequent in children and is correlated with high CNS relapse rate [130]. In addition, roscovitine was recently reported to have strong anti-inflammatory effect [120] and it reduced effectively post treatment neurological sequelae of acute pneumococcal meningitis in mice due to apoptosis of the activated neutrophils in the brain [131]. This knowledge supports future indication of roscovitine in children especially in primary or secondary malignancy and infections of CNS. Unfortunately, scaling down the PK data from adults to pediatrics, has been approved not to be enough predictive for many drugs [90]. In study II, we reported for the first time the age dependent PK of roscovitine in a rat model. The administration of the same dose of roscovitine to 14 days old rat pups and adult rats has resulted in significant difference in PK of roscovitine and its distribution to the brain between the two age groups. The AUC of roscovitine was 22-fold higher and the elimination half-life was 14-fold (7 hr) longer compared to that found in plasma of adult rats (<30 min). This difference in exposure might be due to the immaturity of the CYP450 enzymes responsible for roscovitine metabolism [132]. Roscovitine is metabolized in human mainly by CYP3A4 and CYP2B6 enzymes [78]. Rich and Boobis have shown that many CYP450 enzymes are not fully matured at the age of 2 weeks in rats [133]. Similar situation was also reported in human and CYP3A4 for example approaches the adult full capacity only after first year of life [128].

It is well known that despite enough systemic exposure, most chemotherapeutic agents can not cross the blood brain barrier (BBB) and do not reach the CNS in enough high concentrations to eliminate tumor cells. Surprisingly, for roscovitine, the age did not affect only the PK but also the biodistribution into the brain. Strikingly, we found that roscovitine was highly distributed over the BBB in the pups and the brain exposure in all studied

regions (e.g. hippocampus, cerebral cortex and cerebellum) was 100% of that found in plasma as expressed as AUC brain/AUC plasma. This can be compared to about 25% that has been found in the brain of adult rats which is in agreement with the results reported by Vita et al., where the distribution into the brain was found to be 30% of that found in plasma [72].

The differences observed in brain exposure could be explained by an age-dependent variation in the maturity and function of BBB. Butt et al. have shown that BBB of the rat fully matures 3–4 weeks postnatal [134].

Our results demonstrated that exposure to roscovitine in the plasma and the brain to levels higher than the reported tumor IC₅₀ (10-15 μ M) could be achieved for more than 8 hours in infant rats. However, this desired exposure is not achievable longer than 30 minutes in plasma and brain of adult rats. This could be implemented in the treatment of pediatric malignancies especially for CNS malignancies.

Roscovitine is a potent inhibitor of Cdk5 which has important functions in the developing brain such as neuronal migration [14]. Moreover, Cdk5 up-regulates NMDARs and plays a key role in synaptic plasticity and memory development [135]. In addition, the negative feedback regulation of mitogen activated protein kinases (MAPK) signaling by Cdk5 has been suggested to be important for neuronal survival [19].

Based on the high concentrations of roscovitine found in the brain of pups, we determined its activity to assess the PK/PD relationship between high concentrations and the inhibition of target enzymes. We measured the expression of p35 as an indicator of Cdk5 activity. Inhibition of p35 phosphorylation by Cdk5 stabilizes it and delays its proteasomal degradation [11, 12]. Higher levels of p35 were observed in treated animals until 2 hours. The activity of Cdk5 was recovered reaching the control levels at 6 hr. Surprisingly, the concentrations of roscovitine after 6 hr were high enough to inhibit Cdk5 *in vitro* (IC₅₀ 0.16 μ M). This PK/PD mismatch might be due to different factors such as high intraneuronal ATP concentrations, drug internalization and the short half-life of p35 with subsequent transcription of drug-free protein [11]. Also, non-specific tissue binding was reported to be an important reason for the PK/PD mismatch in the brain [136].

Cdk5 was found to inhibit Erk1/2 phosphorylation by a MEK1 and RasGRF2 mediated mechanism and the inhibition of Cdk5 by roscovitine increased the levels of phosphorylated Erk1/2 (activated) in neuronal cells *in vitro* [19, 137]. We measured the levels of phosphorylated Erk1/2 in different time points and we found an increase in phosphorylated Erk1/2 levels which correlated with the same time course of Cdk5 inhibition (i.e. levels increased at the first 2 hr after administration and returned to control levels after 6 hr). It is noteworthy that measurement of the phosphorylation of Erk1/2 was suggested to be a potential pharmacodynamic marker of roscovitine activity in clinical trials [138].

In view of our results we concluded that roscovitine has a favorable PK profile in young animals and may be considered as a promising candidate for the treatment of primary and secondary brain tumors in pediatric patients. However, more extended and long-term studies are warranted.

5.3 CHRONO-BIO-DISTRIBUTION

Circadian rhythm controls daily biological rhythms including sleep-wake, hormone secretion and metabolism. These rhythms are generated by molecular clocks based on intracellular transcription-translation feedback loops that sustain daily oscillations of gene expression in many cell types. It has been reported that the time of dosing can modify significantly the pharmacokinetics of several classes of drugs including anticancer drugs, due to the rhythmic regulation of most of the physiological processes controlling the ADME processes. It is important to consider circadian rhythms in pharmacokinetics and the responses to therapy in order to design proper protocols for roscovitine administration.

Lurisci et al. have investigated the chronopharmacodynamics of roscovitine in Glasgow osteosarcoma xenografts and found that the administration of roscovitine at ZT19 when the mice are active induced 35% tumor growth inhibition, while administration of roscovitine at ZT3 when the mice are resting induced 55% tumor growth inhibition and better tolerability [68]. In order to address the relation between these results and the pharmacokinetics of roscovitine, we investigated the chronopharmacokinetics and biodistribution of roscovitine in the same mouse strain. Our findings confirmed the dosing time-dependence of roscovitine pharmacokinetics, we have also found that the exposure at ZT3 was 38% higher and elimination half-life was 100% longer

compared to that observed at ZT19. The higher exposure was also found in several organs including kidney (180%), adipose tissue (188%), testis (132%) and lungs (112%). These differences in exposure might explain the improved antitumor activity at ZT3 which was observed by Iurisci et al.

The circadian oscillations in all the ADME processes could contribute to this pharmacokinetics differences [94, 139]. Roscovitine clearance was slower and elimination half life was longer at ZT3, both findings might indicate slower metabolism of roscovitine at the rest time. Moreover, the metabolic ratio of roscovitine was significantly higher at ZT19. To explain these findings, we performed *in vitro* incubation assays with microsomes prepared from liver tissues taken from untreated mice at either ZT3 or ZT19. Our results showed a significant difference in the intrinsic clearance (CL_{int}) value between both circadian times with higher CL_{int} at ZT19. Moreover, no significant difference in microsomal protein levels per gram of liver tissue was found between the two circadian times. All these together, may indicate increased metabolism of roscovitine at ZT19 due to the increased activity of specific metabolizing enzymes rather than an unspecific increase in their proteins expression. Roscovitine is metabolized in the human liver mainly by cytochrome P450 enzymes 3A4 and 2B6 [78]. It has been shown previously that the regulation of CYP3A enzymes is slow and the mRNA of CYP3A enzymes is stable for about 1 day [140]. Thus, circadian variations in CYP3A amount should not be significant [95, 109]. Different mechanisms other than CYP3A synthesis has been described for the oscillations in its activity, such as variability in other physiologic regulators or protein partners like P450 oxidoreductase - provider of the electrons necessary for P450 function- which fluctuates in circadian pattern [95, 109].

Volume of distribution was higher at ZT3 compared to ZT19. The absorption and distribution of drugs depend on many physiological and biochemical processes which are influenced by the circadian rhythm such as cardiac output, organ blood flow, gastric emptying, intestinal transporter activity and the extent of protein binding. In humans, most lipophilic drugs seem to be absorbed faster when the drug is taken in the morning compared with the evening [94] and it has been shown that cardiac output and blood flow distribution to intestinal mucosa increase during the active phase by 30% compared to that found during the rest period [94] and the opposite occur in rodents. Higher C_{max} at

ZT19 may be attributed to increased absorption of roscovitine. This may be due to an increase in cardiac output with higher intestinal mucosal blood flow, changes in gastric emptying and gastric acid secretion or higher uptake transporter activity.

Roscovitine is highly bound to plasma proteins (90-96%) [46, 77]. The highest plasma protein binding in humans occurs in the afternoon and the lowest during the night, meaning there is more bound drug in the body when active [94, 95]. The volume of distribution of roscovitine was lower at ZT19 which is the active period in mice. That could be due to increase in the bound fraction of the drug, which is not distributed readily in the peripheral tissues.

The delivery of roscovitine at ZT3 led to 80% higher exposure to roscovitine in kidney. This finding may be relevant to the clinical development of the drug as a treatment for renal diseases such as proliferative glomerulonephritis [37, 73, 141] and also to minimize or prevent the transient renal toxicities of roscovitine in clinical trials [76]. Shifting of the dosing time could help to increase or decrease the kidney exposure significantly with subsequent higher efficacy or decreased toxicity according to the clinical situation. Further studies about the effect of roscovitine on the renal molecular clock and identification of relevant PD markers in kidney would be very helpful in optimizing the dose of roscovitine.

In contrast to plasma and other organs, liver/plasma AUC ratio was higher at ZT19 compared with ZT3. This might indicate higher first extraction ratio of roscovitine at ZT19 due to increased hepatic blood flow and higher uptake transport (if roscovitine is a substrate for liver uptake transporters) during active periods [139].

Our results show that the pharmacokinetics of roscovitine in male DBF1 mice is significantly affected by circadian rhythm. Higher systemic exposure and more extensive biodistribution occur when roscovitine is administered at ZT3. This can be attributed to a lower rate of metabolism, i.e. lower intrinsic clearance of the drug during the day when the mice are resting. Drug concentrations in some tissues, like kidney, testis and adipose tissue, were high during ZT3 when the mice are resting. The associations between PK parameters and toxicities have been frequently reported in rodent models and in humans [100, 105, 142], that means if similar variations to our findings would be detected in

diurnal mammals like humans, the time of dosing should be carefully considered when using roscovitine clinically.

5.4 ROSCOVITINE ANALOGUES

Roscovitine was introduced as a promising antitumor Cdk_i with good selectivity and high potency. However, the drug has shown modest success in clinical trials due to its pharmacokinetics, especially the short elimination half-life which do not allow effective exposure of tumor cells to roscovitine. Different drug discovery programs have been launched for synthesis and development of second generation analogues of roscovitine, which could have higher potency and better pharmacokinetic profiles.

In study IV, we investigated the biological and pharmacokinetic characteristics of two roscovitine bioisosters named N-&-N1 and N-&-N2. The selectivity profile for Cdk inhibition of both N-&-N analogues was comparable with roscovitine, however, N-&-N1 showed exquisite 2- to 3-fold enhanced potency compared with roscovitine. N-&-N1 was able to inhibit Rb protein phosphorylation in neuroblastoma cell lines. Both analogues were tested for antitumor activity. The compounds were able to induce apoptotic cell death in 6 tumor cell lines. N-&-N1 was 5-6 times more potent (IC₅₀ 5.2 μM) compared to roscovitine (IC₅₀ 28.3 μM) considering tumor cell death induction.

These encouraging results as antitumor *in vitro* were the basis to study the PK of N-&-N1 as an important step in its development and to estimate the proper dose to be used in animal models. Poor pharmacokinetics would counteract the increased biochemical/ cell biology potential of N-&-N1. Suitable, robust and reproducible analytical method for both pre-clinical and clinical studies is of great importance for newly introduced drugs such as Cdk inhibitors that are promising for the treatment of several diseases including cancer.

In order to study the PK of N-&-N1, we developed and validated simple analytical method using HPLC-UV according to the FDA guidelines [110, 112]. Selectivity, linearity, calibration, precision, accuracy and recovery of the method were within acceptable values. Changing the position of N9 in the purine ring has modified the UV absorption range of roscovitine and the best absorption was found at 220 nm, not 292 nm as it is for roscovitine [71]. N-&-N1 has the same elimination half-life as for roscovitine. However, with the increased

potency of N-&-N1 compared to roscovitine, better *in vivo* antitumor activity has been shown [143].

In our last study, we investigated the PK profile of another second generation analogue of roscovitine named CR8 [83]. Recently, CR8 have been shown to have 2-4 folds more potency as a Cdk inhibitor *in vitro* and 50-100 fold more cytotoxic in tumor cell lines [81]. However, this enhanced *in vitro* activity of CR8 needs to be confirmed *in vivo* in animal models prior to further development towards clinical trials. In the present investigation we have developed and validated a new analytical method for the determination of CR8 in plasma and tissue samples. Our data showed that the method is selective and accurate. The acceptance criteria for the validation of the method are well in accordance with internationally accepted criteria [111, 112]. Moreover, the volume required for the analysis was only 50 μ L of plasma, a favorable factor when considering plasma sampling from small laboratory animals.

We implemented this method in the analysis of CR8 in plasma and tissue homogenates of the mice. CR8 was found to have 100% oral bioavailability, which means the drug is suitable for oral route intake and that the first pass effect is negligible. Longer elimination half-life compared to roscovitine (3 hr and 1 hr, respectively, in female Balb/c mice) allow plasma concentrations for more than 10 hours to be far higher than the anti-tumor IC₅₀ values found *in vitro*.

The systemic exposure to roscovitine (expressed as AUC in plasma) in adult animals and in human did not allow a plasma concentration to be maintained above the reported anti-tumor IC₅₀ (15-17 μ M) for more than 1-2 hour, even when the maximum tolerated doses were administered [72, 76] (except in young rats due to immature metabolism as we have shown in the second study). Thus, second generation analogues of roscovitine might, in addition to increased antitumor potency, solve the problem of insufficient exposure observed in roscovitine.

CR8 distributed rapidly to all the peripheral tissues. The highest tissue distribution, as compared to plasma AUC, was found mainly in elimination organs, namely liver (200%) and kidneys (150%). These results encourage the possibility for CR8 to be used in the treatment of liver and kidney tumors since

CR8 was found to induce apoptotic cell death in both hepatic and renal tumors cell lines.

In contrast to roscovitine, CR8 showed higher distribution to the bone marrow (30%) compared to roscovitine (1.5%). Moreover, spleen biodistribution was about 40% of systemic exposure. This distribution pattern to the BM and spleen might encourage the application of CR8 in treatment of leukemia and lymphomas, especially when CR8 showed high cytotoxic activity against leukemic cell lines [81]. However, the high biodistribution to the bone marrow may cause myelosuppression which was not found with roscovitine. Further studies are needed to explore the cytotoxic effect of CR8 on normal hematopoietic progenitors.

We also have shown that CR8 passes the BBB. AUC (brain/plasma) was 15% compared to that reported for roscovitine (30%) [72]. This brain exposure is nevertheless higher than that required for inhibition of CR8 neuronal targets like Cdk5 and CK1 (IC₅₀ values: 0.12 μ M and 0.61 μ M, respectively) [72]. This fact may benefit the drug for further studies in neurodegenerative animal models and brain tumor models.

6. CONCLUSIONS

- Mouse hematopoietic progenitors are inhibited by roscovitine *in vitro* within the same exposure range as malignant cells; however, the cytotoxic effect of roscovitine on hematopoietic progenitors *in vivo* is transient due to inadequate exposure.
- Age-dependent pharmacokinetics of roscovitine was demonstrated in rats. Prolonged systemic and brain exposure to roscovitine occur in young compared to adult rats, which may be due to immature CYP450 enzymes as well as blood brain barrier. Moreover, roscovitine is able to induce transient effect on critical neuronal targets and signaling pathways in the brain of young rats. These results raised the questions if roscovitine can be a candidate for treatment of primary and secondary brain tumors in children? And what are the long term effects of roscovitine therapy on the developing brain?
- The pharmacokinetics of roscovitine in mice is significantly affected by circadian rhythm. Administration of the drug during the resting period led to higher systemic exposure and more extensive biodistribution to organs compared to that observed when the drug was administered during the active period. Slower rate of roscovitine metabolism may contribute to this difference. The time of dosing should be carefully considered when using roscovitine clinically.
- N&N1 is a new bioisoster analogue of roscovitine with improved antitumor activity. Simple HPLC-UV bioanalytical method for determination of N&N1 concentrations was developed and validated. N&N1 pharmacokinetics profile in mice is similar to its analogue roscovitine; however, due its improved potency on tumor cells, better *in vivo* activity on tumor xenografts may be expected.
- CR8 is a second generation analogue of roscovitine. We developed and validated a simple and sensitive HPLC-UV method for the analysis of CR8 in biological matrices. Pharmacokinetic pattern showed 100% bioavailability and long half life, which may allow prolonged systemic exposure higher above IC50 in tumor cell lines. .

7. FUTURE PERSPECTIVES

During the past decade several Cdk inhibitors with activity against both cell cycle Cdk (Cdk1, 2, 7) and transcription Cdk (Cdk7 and Cdk9) have been introduced. Moreover, promising results have been reported supporting the activity of Cdk inhibitor against many diseases including malignancies, glomerulonephritis, neurodegenerative disorders, viral infections, protozoal infections and inflammatory diseases. All together has tremendously increased the interest for both clinical as well as preclinical research about Cdk inhibitors. Roscovitine and its chemically derived analogues showed wide spectrum of activity, and so are expected to be good candidates in cancer therapy and other diseases. However, better *in vivo* activity still depends on the design of pharmacologically superior schedules for the administration of these drugs.

In vitro assays to investigate in details the effect of circadian rhythm on metabolism of roscovitine after multiple dosing schedules, which can be implemented in preclinical and clinical trials [68, 76] would be of great importance. Roscovitine was reported to inhibit its metabolism enzymes *in vitro* [78] while it is capable to induce some metabolic enzymes like UGT1A1 and CYP2B6 in hepatocytes [144] all these together confirm the importance of such experiments in the chronotherapy of roscovitine. Moreover, roscovitine may be a substrate of ABC transporter family such as permeability glycoprotein (P-gp). Studies to illustrate the role of P-gp or other efflux protein would help to predict P-gp-mediated drug interactions [145].

Further investigation of the metabolic pathways involved in the metabolism of roscovitine analogues is a key step towards their development. This involves the identification of the metabolites and their pharmacological activity. More important is to determine the CYP450 responsible for their metabolism in order to avoid drug interaction. Metabolites of these analogues may be active against tumor cells or may cause higher general toxicity. The identification of these metabolites would help to include them in the design of better dosing schedules and to identify the possible drug- drug interactions.

This knowledge will help to understand the effects of Cdk inhibitors on the cellular level and to improve their efficacy [43, 146].

8. ACKNOWLEDGMENT

Sincere thanks and full appreciation to all people who helped me in my PhD. I am sure that no words will be enough to express my feelings and gratitude to everyone who helped me during these 4 years. At the beginning I want to thank the department of laboratory medicine and the department of medicine at Karolinska Institutet and to thank "Sweden" for having such great university.

I would like also to express my gratitude to all the colleagues who helped me to achieve my work, especially to;

Professor Moustapha Hassan, my main supervisor; you are a good scientist with great personality. Thanks for your trust in my abilities and your good help in writing and strategic research decisions, your continuous support and help when ever it was needed... I hope this is the beginning not the end of our journey. "Thanks Prof."

Professor Laurent Meijer, my co-supervisor. It was a great opportunity to work with you. Thank you for your kind words, scientific help and support. I believe that still much I can learn from you... My best wishes for you and "ManRos therapeutics" to find the magic bullet against cancer!

Professor Magnus Ingelman-Sundberg, My co-supervisor; probably we didn't have the chance to work closely together, but still I believe you are one of the remarkable people in your field. Thank you to accept me as your student and to give me your time when ever I ask for it.

Associate Professor Angel Cedazo-Minguiz, My co-supervisor; "Senior" I cannot express my gratitude for you. My experience with you taught me a lot... you are a smart scientist who has a lot to offer to his students... We had many memorable discussions... Simply, working with you is fun and productive...

Associate professor, Zuzana Hassan, our group leader and co-author; you have the success recipe ... Strong personality, determination, the desire for challenging, great abilities and systematic thinking.. Thank you for lending me your critical eyes!!!

Dr.Ylva Terelius, my co-author, thank you very much for the help and guidance you provided to me in the field of drug metabolism despite of your very busy time.

Professor Jan Bolinder Head of the department of medicine and **Professor Lennart Eriksson**, head of the department of laboratory medicine. Thank you for giving me the opportunity to pursue my PhD at KI.

Professor Alaa El-Din Saad Abdel-Hamid, My professor of clinical pathology at **Suez Canal university**, Thanks for everything... you introduced me to Professor Moustapha, you stand by my side step by step, you provided me

with your support and you did whatever you can to make my dream come true. I will be always grateful for you.

Professor Sobhi Elshishi, Head of Community medicine department at Suez Canal University. You encouraged me to get my PhD and you helped me a lot. Thank you!

Professor Francis Levi, and **Elisabeth Filipski** from the "Chronobiology and cancer group" and my co-authors, you added a lot to the knowledge about circadian rhythm and its effects on cancer. Thanks for the fruitful collaboration.

Karyma Bettayeb, my co-author and all the members of "**protein phosphorylation and human diseases**" group at Station Biologique, Roscoff. Good luck.

My friends and collaborators at Astra-Zeneca, especially **Professor Mohammad Abdel-Rehim**, thanks for your generous help! **Patricia Jimenez**, my co-author for her excellent work with brain dissection.

I would like to thank all my past and present colleagues in the experimental cancer medicine (ECM) group;

Christina Hammarstedt, "Tina" you introduced me to our lab, and you smoothed my beginning in the group. Good luck for you and **Mikae. Behnam Sadeghi**, our "lion"!! you were always kind and helpful, special thanks for your help in the animal experiments, I learned a lot from you and we had beautiful memories. My best wishes for your scientific future and for your lovely family. **Parvaneh Afsharian**, thanks for your help in chromatography, and for being always eager to help. We really missed you here! **Rana Said**, my first teacher in chromatography, my dear friend, and jebreel's aunt. Thanks for being there for us. I am really grateful for you. You are smart and kind girl and hopefully the best for you is not yet. **Sulaiman Al-Hashmi**, "Solom", my sweet omani friend. It was pleasure having you in our group, you are generous, cheerful and understanding person and you have very good scientific thinking. Good luck in your defense. **Hairong Song**, my co-author and clever girl; wherever you are now, I hope the success will be your partner. **Mona Fares**, my egyptian colleague, you are a good model for a hard worker with a good heart. I wish you and **Mohammad Haloos** all the best. **Donna Lui**, my irish student and **Brain Morrissey**, you introduced to me the warm Irish personality. I enjoyed our discussions. All the best for your future. **Gayane Avetisyan**, Good luck. **Ladan**, our new student, smart and kind girl, Best wishes in all the life pathway!

Sincere thanks and best wishes for my friends and all the past and present colleagues at NOVUM; **Hamdy Omar**, "My partner", our brotherhood will be forever. All the best for you and your kind family. **Mohammad Saleem**, Good personality and wonderful sense of humor. I know you will get what you want "God willing". **Rami Genead**, clever boy! Good luck for your future. **Eman Zaghlol**, ambitious and hard worker; be sure you will be rewarded by the end.

My friends at hematology lab; **Monica jansson**, great personality, open mind and kind heart, I think you can be ambassador for Sweden! **Lalla Forsblom**, respectful personality and cheerful. **Birgitta Stellan and Mari Gilliam**, the lovely couple with lovely smile! **Ulrika felldin, Ann Svensson, Emma Emanuelsson**. Warm, kind and funny. **Maryam Nikpour**, thanks for your help and lovely discussion. **Mohsen karimi**, always nice to see you, **Evren Alici**, I wish you bright future, **Tolga Sutlu**, hello always. **Maria Cardona** and **Jose Arteaga**, it's my pleasure to know you, all the best from my heart!

Alexandra Treshcow, beautiful smile! it was nice to meet your kind family, good luck in your business and life. **Christian Unger**, Good luck. **Abdalla Jama, Hossain Nawaz, Beston Nore** and **Hossain Alamdar**, thanks and good luck! **Fariel and Dr. Faheem**, respectful and polite family, my best regards and keep in touch. **Agneta** and **Eva** from the cardiology group, Best wishes.

Special regards to my friends from Chile, **Evan Romero** at NMR, your smile always bring hope for me, thanks for the nice time we exchanged opinions and memories and for your eagerness to collaborate and help. **Hernan Concha**, open mind, friendly and kind. "maa elsalama". **Edgardo Faune**. You facilitated our work at KI. Thanks.

My Egyptian friends at KI, **Dr. Essam Mohammad**, I learned a lot from you, you have wise thinking and very high sympathy. We all missed you! Congratulation for the cardio thoracic board and good luck for your future. **Mohammad Yosri, sally** and **jannah**. We had brief time together, however it was very nice. I wish you the best.

Fahad Al-Zadjali and **Abdullah AlManiri**, my omani brothers. I am lucky to know you thanks to Sulaiman. Words cannot describe the nice time we had together. I wish we be close forever. Good luck for your defenses and the best wishes for your families.

Dr. Lauy Al-Anati, kind, generous and trusty palastinian "Zalamah" and professional grill man. Thank you brother and best wishes.

The group of Angel at NVS, **Laura Mateos-Montejo, Nodi Dehvari, Anna Sandebring, Susanne Akterin, Patxi Gil-Bea** and **Monica Perez-Manso**. I had with you my best moments at KI, thanks for your endless help and troubleshooting. I wish you all the best in your future.

Professor Elke Shweda and her group, **Brigitte Twelkmeyer, Mikael Enskog, Varvara Vitiazeva** and **Susana Lundstrom**. We had wonderful trips together, and I always enjoyed your company and humor. Special thanks to **Brigitte** for her continuous help and for introducing the tandem mass spectrometry for me.

My lovely Sudanese friends at KI, **Mohamad Hamza, Hossam Nour** and **Zafer**, we had nice time together, you are best representative of the kindness of Sudanese people!

Sincere thanks and appreciation to all the staff of the clinical research center "KFC"; especially to **Hanna Eriksson**, you are kind, cheerful and helpful always. Thank you. **Åke Ellin**, your instant help with any technical need especially UV-VIS scan was very useful, thank you. **Lotti, Agneta Nelsson, Kirsti, Nelson Murale, Gladis and Isa innecki**. Many thanks as you provided us with the best environment to work with beautiful smile. **Mikael Gradin** and **Jill Gradin**, my host family during my first year, thank you for your help to me and my family and for the smooth introduction to the Swedish culture and life style.

Marita Ward, you are always cheerful, helpful and kind hearted. Thank you. **Fredrick**, our IT coordinator at Labmed department. You are professional troubleshooter. Thanks for your help. **Berit Lecomte**, "Merci Beaucoup"

To all the animal facility staff, thanks for your help which was never limited. Special thanks to **Nattan, Mikael, Kristina** and **Jose**

Adam and **Amir Hassan**, Thanks for our nice discussions, all the best for future.

To my Egyptian friends, **Mohamad shabrawy, ahmed Gharbawy, Mohamad shatta, sherief Khattab, Sameh** and **Mohammad Bahnasawy, Khaled Salah Eldin, Adel Elsherief, Mohammad Issa** and all my friends who I have been attached to them for being lovely and kind with me.

To my lovely spouse, **Souad**, You and my son **Jebreel** made my life meaningful, you always stand by my back, warm up my life and most importantly, keep me safe from starvation with your tasty recipes! Thank you for all your support, sympathy and kindness. I pray always that our life will be full of love and cordiality.

To My Father, **Dr. Hamed Sallam**. You were a great doctor who gave his job the first priority always., I promise you that I will do my best to carry on your work and to make the memory of your achievements alive, you will be always that star that I'm looking high to it . To my mother, **Dr Samia Elmolla**, you are an ideal mother, who balanced between her work and her home. Thank you very much for all what you have done and still doing for us, you are the most valuable person in my life! I dedicate my work for youplease accept it

To my sister **Dr. Nahla** and family (**Dr. Hisham, Salma** and **Jannah**). And to my pretty sister **Aliaa**. I love you so much. Special thanks full of love and appreciation to all my big family in Egypt and Belgium.

Full appreciation to my home university "**Suez Canal University**" and to all my professors and supervisors.

These investigations were made possible due to the kind contribution from: Swedish Children Cancer Society "Barncancer Fonden", Swedish Cancer Foundation "Cancer Fonden", Karolinska Institutet grant and travel grants from Radiumhemmets forskningsfonder.

9. REFERENCES

1. Cohen, P., *Protein kinases--the major drug targets of the twenty-first century?* Nat Rev Drug Discov, 2002. **1**(4): p. 309-15.
2. Malumbres, M. and M. Barbacid, *Mammalian cyclin-dependent kinases*. Trends Biochem Sci, 2005. **30**(11): p. 630-41.
3. Santamaria, D., et al., *Cdk1 is sufficient to drive the mammalian cell cycle*. Nature, 2007. **448**(7155): p. 811-5.
4. Meijer, L., et al., *Biochemical and cellular effects of roscovitine, a potent and selective inhibitor of the cyclin-dependent kinases cdc2, cdk2 and cdk5*. Eur J Biochem, 1997. **243**(1-2): p. 527-36.
5. Morgan, D.O., *Cyclin-dependent kinases: engines, clocks, and microprocessors*. Annu Rev Cell Dev Biol, 1997. **13**: p. 261-91.
6. Garriga, J. and X. Grana, *Cellular control of gene expression by T-type cyclin/CDK9 complexes*. Gene, 2004. **337**: p. 15-23.
7. Loyer, P., et al., *Role of CDK/cyclin complexes in transcription and RNA splicing*. Cell Signal, 2005. **17**(9): p. 1033-51.
8. Elmlund, H., et al., *The cyclin-dependent kinase 8 module sterically blocks Mediator interactions with RNA polymerase II*. Proc Natl Acad Sci U S A, 2006. **103**(43): p. 15788-93.
9. Trembley, J.H., et al., *Casein kinase 2 interacts with cyclin-dependent kinase 11 (CDK11) in vivo and phosphorylates both the RNA polymerase II carboxyl-terminal domain and CDK11 in vitro*. J Biol Chem, 2003. **278**(4): p. 2265-70.
10. Cruz, J.C. and L.H. Tsai, *A Jekyll and Hyde kinase: roles for Cdk5 in brain development and disease*. Curr Opin Neurobiol, 2004. **14**(3): p. 390-4.
11. Nikolic, M. and L.H. Tsai, *Activity and regulation of p35/Cdk5 kinase complex*. Methods Enzymol, 2000. **325**: p. 200-13.
12. Patrick, G.N., et al., *p35, the neuronal-specific activator of cyclin-dependent kinase 5 (Cdk5) is degraded by the ubiquitin-proteasome pathway*. J Biol Chem, 1998. **273**(37): p. 24057-64.
13. Patrick, G.N., et al., *Conversion of p35 to p25 deregulates Cdk5 activity and promotes neurodegeneration*. Nature, 1999. **402**(6762): p. 615-22.
14. Dhavan, R. and L.H. Tsai, *A decade of CDK5*. Nat Rev Mol Cell Biol, 2001. **2**(10): p. 749-59.
15. Angelo, M., F. Plattner, and K.P. Giese, *Cyclin-dependent kinase 5 in synaptic plasticity, learning and memory*. J Neurochem, 2006. **99**(2): p. 353-70.
16. Bibb, J.A., *Role of Cdk5 in neuronal signaling, plasticity, and drug abuse*. Neurosignals, 2003. **12**(4-5): p. 191-9.
17. Nguyen, C. and J.A. Bibb, *Cdk5 and the mystery of synaptic vesicle endocytosis*. J Cell Biol, 2003. **163**(4): p. 697-9.

18. Tomizawa, K., et al., *Cdk5/p35 regulates neurotransmitter release through phosphorylation and downregulation of P/Q-type voltage-dependent calcium channel activity*. J Neurosci, 2002. **22**(7): p. 2590-7.
19. Zheng, Y.L., et al., *Cdk5 Modulation of mitogen-activated protein kinase signaling regulates neuronal survival*. Mol Biol Cell, 2007. **18**(2): p. 404-13.
20. Wang, C.X., et al., *Cyclin-dependent kinase-5 prevents neuronal apoptosis through ERK-mediated upregulation of Bcl-2*. Cell Death Differ, 2006. **13**(7): p. 1203-12.
21. Lazaro, J.B., et al., *Cyclin dependent kinase 5, cdk5, is a positive regulator of myogenesis in mouse C2 cells*. J Cell Sci, 1997. **110** (Pt 10): p. 1251-60.
22. Canduri, F., et al., *CDK9 a potential target for drug development*. Med Chem, 2008. **4**(3): p. 210-8.
23. Zhang, Q., et al., *Cyclin-dependent kinase 5 is associated with apoptotic cell death during development and tissue remodeling*. Dev Biol, 1997. **183**(2): p. 222-33.
24. Hakem, A., et al., *The cyclin-dependent kinase Cdk2 regulates thymocyte apoptosis*. J Exp Med, 1999. **189**(6): p. 957-68.
25. Hiromura, K., et al., *The subcellular localization of cyclin dependent kinase 2 determines the fate of mesangial cells: role in apoptosis and proliferation*. Oncogene, 2002. **21**(11): p. 1750-8.
26. Perez de Castro, I., G. de Carcer, and M. Malumbres, *A census of mitotic cancer genes: new insights into tumor cell biology and cancer therapy*. Carcinogenesis, 2007. **28**(5): p. 899-912.
27. Ortega, S., M. Malumbres, and M. Barbacid, *Cyclin D-dependent kinases, INK4 inhibitors and cancer*. Biochim Biophys Acta, 2002. **1602**(1): p. 73-87.
28. Strock, C.J., et al., *Cyclin-dependent kinase 5 activity controls cell motility and metastatic potential of prostate cancer cells*. Cancer Res, 2006. **66**(15): p. 7509-15.
29. Goodyear, S. and M.C. Sharma, *Roscovitine regulates invasive breast cancer cell (MDA-MB231) proliferation and survival through cell cycle regulatory protein cdk5*. Exp Mol Pathol, 2007. **82**(1): p. 25-32.
30. Plattner, F., M. Angelo, and K.P. Giese, *The roles of cyclin-dependent kinase 5 and glycogen synthase kinase 3 in tau hyperphosphorylation*. J Biol Chem, 2006. **281**(35): p. 25457-65.
31. Shelton, S.B. and G.V. Johnson, *Cyclin-dependent kinase-5 in neurodegeneration*. J Neurochem, 2004. **88**(6): p. 1313-26.
32. Wang, J., et al., *Cdk5 activation induces hippocampal CA1 cell death by directly phosphorylating NMDA receptors*. Nat Neurosci, 2003. **6**(10): p. 1039-47.
33. Liu, L., et al., *Cyclin-dependent kinase inhibitors block leukocyte adhesion and migration*. J Immunol, 2008. **180**(3): p. 1808-17.

34. Matushansky, I., F. Radparvar, and A.I. Skoultschi, *Reprogramming leukemic cells to terminal differentiation by inhibiting specific cyclin-dependent kinases in G1*. Proc Natl Acad Sci U S A, 2000. **97**(26): p. 14317-22.
35. Leitch, A., C. Haslett, and A. Rossi, *Cyclin-dependent kinase inhibitor drugs as potential novel anti-inflammatory and pro-resolution agents*. Br J Pharmacol, 2009.
36. Hussain, S.P. and C.C. Harris, *Inflammation and cancer: an ancient link with novel potentials*. Int J Cancer, 2007. **121**(11): p. 2373-80.
37. Obligado, S.H., et al., *CDK/GSK-3 inhibitors as therapeutic agents for parenchymal renal diseases*. Kidney Int, 2008. **73**(6): p. 684-90.
38. Agbottah, E., et al., *Antiviral activity of CYC202 in HIV-1-infected cells*. J Biol Chem, 2005. **280**(4): p. 3029-42.
39. Schang, L.M., et al., *Pharmacological cyclin-dependent kinase inhibitors inhibit replication of wild-type and drug-resistant strains of herpes simplex virus and human immunodeficiency virus type 1 by targeting cellular, not viral, proteins*. J Virol, 2002. **76**(15): p. 7874-82.
40. Cujec, T.P., et al., *The HIV transactivator TAT binds to the CDK-activating kinase and activates the phosphorylation of the carboxy-terminal domain of RNA polymerase II*. Genes Dev, 1997. **11**(20): p. 2645-57.
41. Knockaert, M., P. Greengard, and L. Meijer, *Pharmacological inhibitors of cyclin-dependent kinases*. Trends Pharmacol Sci, 2002. **23**(9): p. 417-25.
42. De Azevedo, W.F., et al., *Inhibition of cyclin-dependent kinases by purine analogues: crystal structure of human cdk2 complexed with roscovitine*. Eur J Biochem, 1997. **243**(1-2): p. 518-26.
43. Bach, S., et al., *Roscovitine targets, protein kinases and pyridoxal kinase*. J Biol Chem, 2005. **280**(35): p. 31208-19.
44. Tang, L., et al., *Crystal structure of pyridoxal kinase in complex with roscovitine and derivatives*. J Biol Chem, 2005. **280**(35): p. 31220-9.
45. McClue, S.J., et al., *In vitro and in vivo antitumor properties of the cyclin dependent kinase inhibitor CYC202 (R-roscovitine)*. Int J Cancer, 2002. **102**(5): p. 463-8.
46. Raynaud, F.I., et al., *Cassette dosing pharmacokinetics of a library of 2,6,9-trisubstituted purine cyclin-dependent kinase 2 inhibitors prepared by parallel synthesis*. Mol Cancer Ther, 2004. **3**(3): p. 353-62.
47. Bloom, J. and M. Pagano, *Deregulated degradation of the cdk inhibitor p27 and malignant transformation*. Semin Cancer Biol, 2003. **13**(1): p. 41-7.
48. Zhang, G.J., et al., *Bioluminescent imaging of Cdk2 inhibition in vivo*. Nat Med, 2004. **10**(6): p. 643-8.
49. Krude, T., *Initiation of human DNA replication in vitro using nuclei from cells arrested at an initiation-competent state*. J Biol Chem, 2000. **275**(18): p. 13699-707.

50. Matsumoto, Y., K. Hayashi, and E. Nishida, *Cyclin-dependent kinase 2 (Cdk2) is required for centrosome duplication in mammalian cells*. *Curr Biol*, 1999. **9**(8): p. 429-32.
51. Sirri, V., D. Hernandez-Verdun, and P. Roussel, *Cyclin-dependent kinases govern formation and maintenance of the nucleolus*. *J Cell Biol*, 2002. **156**(6): p. 969-81.
52. Payton, M., et al., *Discovery and evaluation of dual CDK1 and CDK2 inhibitors*. *Cancer Res*, 2006. **66**(8): p. 4299-308.
53. Raynaud, F.I., et al., *In vitro and in vivo pharmacokinetic-pharmacodynamic relationships for the trisubstituted aminopurine cyclin-dependent kinase inhibitors olomoucine, bohemine and CYC202*. *Clin Cancer Res*, 2005. **11**(13): p. 4875-87.
54. Wesierska-Gadek, J., M. Gueorguieva, and M. Horky, *Roscovitine-induced up-regulation of p53AIP1 protein precedes the onset of apoptosis in human MCF-7 breast cancer cells*. *Mol Cancer Ther*, 2005. **4**(1): p. 113-24.
55. Wesierska-Gadek, J., et al., *Roscovitine up-regulates p53 protein and induces apoptosis in human HeLaS(3) cervix carcinoma cells*. *J Cell Biochem*, 2008. **105**(5): p. 1161-71.
56. Lacrima, K., et al., *In vitro activity of cyclin-dependent kinase inhibitor CYC202 (Seliciclib, R-roscovitine) in mantle cell lymphomas*. *Ann Oncol*, 2005. **16**(7): p. 1169-76.
57. MacCallum, D.E., et al., *Seliciclib (CYC202, R-Roscovitine) induces cell death in multiple myeloma cells by inhibition of RNA polymerase II-dependent transcription and down-regulation of Mcl-1*. *Cancer Res*, 2005. **65**(12): p. 5399-407.
58. Alvi, A.J., et al., *A novel CDK inhibitor, CYC202 (R-roscovitine), overcomes the defect in p53-dependent apoptosis in B-CLL by down-regulation of genes involved in transcription regulation and survival*. *Blood*, 2005. **105**(11): p. 4484-91.
59. Mohapatra, S., et al., *Accumulation of p53 and reductions in XIAP abundance promote the apoptosis of prostate cancer cells*. *Cancer Res*, 2005. **65**(17): p. 7717-23.
60. Kim, E.H., et al., *Roscovitine sensitizes glioma cells to TRAIL-mediated apoptosis by downregulation of survivin and XIAP*. *Oncogene*, 2004. **23**(2): p. 446-56.
61. Wesierska-Gadek, J., M. Gueorguieva, and M. Horky, *Dual action of cyclin-dependent kinase inhibitors: induction of cell cycle arrest and apoptosis. A comparison of the effects exerted by roscovitine and cisplatin*. *Pol J Pharmacol*, 2003. **55**(5): p. 895-902.
62. Meijer L, B.K., Galons H., *Roscovitine (CYC202, Seliciclib)*. In: *Smith PJ and Yue E (eds). Monographs on Enzyme*

- Inhibitors. CDK Inhibitors and their Potential as Anti-Tumor Agents.* CRC Press, Taylor & Francis: Boca Raton, Fl. Vol. 2 chapter 9. 2006. 187-226.
63. Lu, W., et al., *Activation of p53 by roscovitine-mediated suppression of MDM2 expression.* *Oncogene*, 2001. **20**(25): p. 3206-16.
 64. Abal, M., et al., *Enhanced sensitivity to irinotecan by Cdk1 inhibition in the p53-deficient HT29 human colon cancer cell line.* *Oncogene*, 2004. **23**(9): p. 1737-44.
 65. Lambert, L.A., et al., *Autophagy: a novel mechanism of synergistic cytotoxicity between doxorubicin and roscovitine in a sarcoma model.* *Cancer Res*, 2008. **68**(19): p. 7966-74.
 66. Coley, H.M., et al., *The effects of the CDK inhibitor seliciclib alone or in combination with cisplatin in human uterine sarcoma cell lines.* *Gynecol Oncol*, 2007. **105**(2): p. 462-9.
 67. Coley, H.M., C.F. Shotton, and H. Thomas, *Seliciclib (CYC202; r-roscovitine) in combination with cytotoxic agents in human uterine sarcoma cell lines.* *Anticancer Res*, 2007. **27**(1A): p. 273-8.
 68. Iurisci, I., et al., *Improved tumor control through circadian clock induction by Seliciclib, a cyclin-dependent kinase inhibitor.* *Cancer Res*, 2006. **66**(22): p. 10720-8.
 69. Tirado, O.M., S. Mateo-Lozano, and V. Notario, *Roscovitine is an effective inducer of apoptosis of Ewing's sarcoma family tumor cells in vitro and in vivo.* *Cancer Res*, 2005. **65**(20): p. 9320-7.
 70. Maggiorella, L., et al., *Enhancement of radiation response by roscovitine in human breast carcinoma in vitro and in vivo.* *Cancer Res*, 2003. **63**(10): p. 2513-7.
 71. Vita, M., et al., *Analysis of roscovitine using novel high performance liquid chromatography and UV-detection method: pharmacokinetics of roscovitine in rat.* *J Pharm Biomed Anal*, 2004. **34**(2): p. 425-31.
 72. Vita, M., et al., *Tissue distribution, pharmacokinetics and identification of roscovitine metabolites in rat.* *Eur J Pharm Sci*, 2005. **25**(1): p. 91-103.
 73. Gherardi, D., et al., *Reversal of collapsing glomerulopathy in mice with the cyclin-dependent kinase inhibitor CYC202.* *J Am Soc Nephrol*, 2004. **15**(5): p. 1212-22.
 74. Nutley, B.P., et al., *Metabolism and pharmacokinetics of the cyclin-dependent kinase inhibitor R-roscovitine in the mouse.* *Mol Cancer Ther*, 2005. **4**(1): p. 125-39.
 75. de la Motte, S. and A. Gianella-Borradori, *Pharmacokinetic model of R-roscovitine and its metabolite in healthy male subjects.* *Int J Clin Pharmacol Ther*, 2004. **42**(4): p. 232-9.

76. Benson, C., et al., *A phase I trial of the selective oral cyclin-dependent kinase inhibitor seliciclib (CYC202; R-Roscovotine), administered twice daily for 7 days every 21 days.* Br J Cancer, 2007. **96**(1): p. 29-37.
77. Vita, M., et al., *Stability, pKa and plasma protein binding of roscovotine.* J Chromatogr B Analyt Technol Biomed Life Sci, 2005. **821**(1): p. 75-80.
78. McClue, S.J. and I. Stuart, *Metabolism of the Trisubstituted Purine Cyclin-Dependent Kinase Inhibitor Seliciclib (R-Roscovotine) in Vitro and in Vivo.* Drug Metab Dispos, 2007.
79. Cervenkova, K., et al., *In vitro glycosidation potential towards olomoucine-type cyclin-dependent kinase inhibitors in rodent and primate microsomes.* Physiol Res, 2003. **52**(4): p. 467-74.
80. Fischer, P.M. and A. Gianella-Borradori, *Recent progress in the discovery and development of cyclin-dependent kinase inhibitors.* Expert Opin Investig Drugs, 2005. **14**(4): p. 457-77.
81. Bettayeb, K., et al., *CR8, a potent and selective, roscovotine-derived inhibitor of cyclin-dependent kinases.* Oncogene, 2008. **27**(44): p. 5797-807.
82. Bettayeb, K., et al., *Meriolins, a new class of cell death inducing kinase inhibitors with enhanced selectivity for cyclin-dependent kinases.* Cancer Res, 2007. **67**(17): p. 8325-34.
83. Oumata, N., et al., *Roscovotine-derived, dual-specificity inhibitors of cyclin-dependent kinases and casein kinases I.* J Med Chem, 2008. **51**(17): p. 5229-42.
84. Lin, J.H. and A.Y. Lu, *Role of pharmacokinetics and metabolism in drug discovery and development.* Pharmacol Rev, 1997. **49**(4): p. 403-49.
85. Meibohm, B. and H. Derendorf, *Pharmacokinetic/pharmacodynamic studies in drug product development.* J Pharm Sci, 2002. **91**(1): p. 18-31.
86. Holford, N.H., *Target concentration intervention: beyond Y2K.* Br J Clin Pharmacol, 2001. **52 Suppl 1**: p. 55S-59S.
87. Hassan, M., et al., *Busulphan kinetics and limited sampling model in children with leukemia and inherited disorders.* Bone Marrow Transplant, 1996. **18**(5): p. 843-50.
88. de Jonge, M.E., et al., *Individualised cancer chemotherapy: strategies and performance of prospective studies on therapeutic drug monitoring with dose adaptation: a review.* Clin Pharmacokinet, 2005. **44**(2): p. 147-73.
89. van den Bongard, H.J., et al., *Pharmacokinetically guided administration of chemotherapeutic agents.* Clin Pharmacokinet, 2000. **39**(5): p. 345-67.
90. Bjorkman, S., *Prediction of cytochrome p450-mediated hepatic drug clearance in neonates, infants and children : how accurate are available scaling methods?* Clin Pharmacokinet, 2006. **45**(1): p. 1-11.

91. Bjorkman, S., *Prediction of drug disposition in infants and children by means of physiologically based pharmacokinetic (PBPK) modelling: theophylline and midazolam as model drugs*. Br J Clin Pharmacol, 2005. **59**(6): p. 691-704.
92. Domingo, J.L., *Cobalt in the environment and its toxicological implications*. Rev Environ Contam Toxicol, 1989. **108**: p. 105-32.
93. Ette, E.I. and P.J. Williams, *Population pharmacokinetics I: background, concepts, and models*. Ann Pharmacother, 2004. **38**(10): p. 1702-6.
94. Baraldo, M., *The influence of circadian rhythms on the kinetics of drugs in humans*. Expert Opin Drug Metab Toxicol, 2008. **4**(2): p. 175-92.
95. Levi, F. and U. Schibler, *Circadian rhythms: mechanisms and therapeutic implications*. Annu Rev Pharmacol Toxicol, 2007. **47**: p. 593-628.
96. Innominato, P.F., et al., *Circadian rhythm in rest and activity: a biological correlate of quality of life and a predictor of survival in patients with metastatic colorectal cancer*. Cancer Res, 2009. **69**(11): p. 4700-7.
97. Filipski, E., et al., *Effects of chronic jet lag on tumor progression in mice*. Cancer Res, 2004. **64**(21): p. 7879-85.
98. Filipski, E., et al., *Disruption of circadian coordination accelerates malignant growth in mice*. Pathol Biol (Paris), 2003. **51**(4): p. 216-9.
99. Filipski, E., X.M. Li, and F. Levi, *Disruption of circadian coordination and malignant growth*. Cancer Causes Control, 2006. **17**(4): p. 509-14.
100. Levi, F., et al., *Implications of circadian clocks for the rhythmic delivery of cancer therapeutics*. Philos Transact A Math Phys Eng Sci, 2008. **366**(1880): p. 3575-98.
101. Altinok, A., F. Levi, and A. Goldbeter, *Identifying mechanisms of chronotolerance and chronoefficacy for the anticancer drugs 5-fluorouracil and oxaliplatin by computational modeling*. Eur J Pharm Sci, 2009. **36**(1): p. 20-38.
102. Filipski, E., et al., *Persistent twenty-four hour changes in liver and bone marrow despite suprachiasmatic nuclei ablation in mice*. Am J Physiol Regul Integr Comp Physiol, 2004. **287**(4): p. R844-51.
103. Gholam, D., et al., *Chronomodulated irinotecan, oxaliplatin, and leucovorin-modulated 5-Fluorouracil as ambulatory salvage therapy in patients with irinotecan- and oxaliplatin-resistant metastatic colorectal cancer*. Oncologist, 2006. **11**(10): p. 1072-80.
104. Levi, F., *Chronotherapeutics: the relevance of timing in cancer therapy*. Cancer Causes Control, 2006. **17**(4): p. 611-21.
105. Mormont, M.C. and F. Levi, *Cancer chronotherapy: principles, applications, and perspectives*. Cancer, 2003. **97**(1): p. 155-69.
106. Karlgren, M., S. Miura, and M. Ingelman-Sundberg, *Novel extrahepatic cytochrome P450s*. Toxicol Appl Pharmacol, 2005. **207**(2 Suppl): p. 57-61.

107. Marks, D.B., A.D. Marks, and C.M. Smith, *Basic Clinical Biochemistry: a clinical approach*. 1996: Williams & Wilkins.
108. Gibson, G. and P. Skett, *Introduction to Drug Metabolism*. 3rd ed. 2001: Nelson Thornes.
109. Gachon, F., et al., *The circadian PAR-domain basic leucine zipper transcription factors DBP, TEF, and HLF modulate basal and inducible xenobiotic detoxification*. *Cell Metab*, 2006. **4**(1): p. 25-36.
110. Bressolle, F., M. Bromet-Petit, and M. Audran, *Validation of liquid chromatographic and gas chromatographic methods. Applications to pharmacokinetics*. *J Chromatogr B Biomed Appl*, 1996. **686**(1): p. 3-10.
111. Shah, V.P., et al., *Analytical methods validation: bioavailability, bioequivalence and pharmacokinetic studies. Conference report*. *Eur J Drug Metab Pharmacokinet*, 1991. **16**(4): p. 249-55.
112. Shah, V.P., et al., *Bioanalytical method validation--a revisit with a decade of progress*. *Pharm Res*, 2000. **17**(12): p. 1551-7.
113. Hartmann, C., et al., *Validation of bioanalytical chromatographic methods*. *J Pharm Biomed Anal*, 1998. **17**(2): p. 193-218.
114. Karnes, H.T. and C. March, *Precision, accuracy, and data acceptance criteria in biopharmaceutical analysis*. *Pharm Res*, 1993. **10**(10): p. 1420-6.
115. Afsharian, P., et al., *The effect of repeated administration of cyclophosphamide on cytochrome P450 2B in rats*. *Clin Cancer Res*, 2007. **13**(14): p. 4218-24.
116. Lofgren, S., et al., *Generation of mice transgenic for human CYP2C18 and CYP2C19: characterization of the sexually dimorphic gene and enzyme expression*. *Drug Metab Dispos*, 2008. **36**(5): p. 955-62.
117. Lowry, O.H., et al., *Protein measurement with the Folin phenol reagent*. *J Biol Chem*, 1951. **193**(1): p. 265-75.
118. Meijer, L. and E. Raymond, *Roscovitine and other purines as kinase inhibitors. From starfish oocytes to clinical trials*. *Acc Chem Res*, 2003. **36**(6): p. 417-25.
119. Phelps, M.A., et al., *Clinical response and pharmacokinetics from a phase I study of an active dosing schedule of flavopiridol in relapsed chronic lymphocytic leukemia*. *Blood*, 2009. **113**(12): p. 2637-45.
120. Rossi, A.G., et al., *Cyclin-dependent kinase inhibitors enhance the resolution of inflammation by promoting inflammatory cell apoptosis*. *Nat Med*, 2006. **12**(9): p. 1056-64.
121. Duffin, R., et al., *The CDK inhibitor, R-roscovitine, promotes eosinophil apoptosis by down-regulation of Mcl-1*. *FEBS Lett*, 2009. **583**(15): p. 2540-6.
122. Li, L., et al., *The cyclin dependent kinase inhibitor (R)-roscovitine prevents alloreactive T cell clonal expansion and protects against acute GvHD*. *Cell Cycle*, 2009. **8**(11): p. 1794 - 1802.

123. Corazza, F., et al., *Bone marrow stroma damage induced by chemotherapy for acute lymphoblastic leukemia in children*. *Pediatr Res*, 2004. **55**(1): p. 152-8.
124. Hassan, M., et al., *Pharmacokinetic and metabolic studies of high-dose busulphan in adults*. *Eur J Clin Pharmacol*, 1989. **36**(5): p. 525-30.
125. Hassan, Z., M. Hassan, and E. Hellstrom-Lindberg, *The pharmacodynamic effect of busulfan in the P39 myeloid cell line in vitro*. *Leukemia*, 2001. **15**(8): p. 1240-7.
126. Hassan, Z., et al., *The effect of modulation of glutathione cellular content on busulphan-induced cytotoxicity on hematopoietic cells in vitro and in vivo*. *Bone Marrow Transplant*, 2002. **30**(3): p. 141-7.
127. Daldrup-Link, H.E., et al., *Assessing permeability alterations of the blood-bone marrow barrier due to total body irradiation: in vivo quantification with contrast enhanced magnetic resonance imaging*. *Bone Marrow Transplant*, 2000. **25**(1): p. 71-8.
128. Alcorn, J. and P.J. McNamara, *Pharmacokinetics in the newborn*. *Adv Drug Deliv Rev*, 2003. **55**(5): p. 667-86.
129. Yu, C., et al., *The lethal effects of pharmacological cyclin-dependent kinase inhibitors in human leukemia cells proceed through a phosphatidylinositol 3-kinase/Akt-dependent process*. *Cancer Res*, 2003. **63**(8): p. 1822-33.
130. Wellwood, J. and K. Taylor, *Central nervous system prophylaxis in haematological malignancies*. *Intern Med J*, 2002. **32**(5-6): p. 252-8.
131. Koedel, U., et al., *Apoptosis is essential for neutrophil functional shutdown and determines tissue damage in experimental pneumococcal meningitis*. *PLoS Pathog*, 2009. **5**(5): p. e1000461.
132. Nouws, J.F., *Pharmacokinetics in immature animals: a review*. *J Anim Sci*, 1992. **70**(11): p. 3627-34.
133. Rich, K.J. and A.R. Boobis, *Expression and inducibility of P450 enzymes during liver ontogeny*. *Microsc Res Tech*, 1997. **39**(5): p. 424-35.
134. Butt, A.M., H.C. Jones, and N.J. Abbott, *Electrical resistance across the blood-brain barrier in anaesthetized rats: a developmental study*. *J Physiol*, 1990. **429**: p. 47-62.
135. Li, B.S., et al., *Regulation of NMDA receptors by cyclin-dependent kinase-5*. *Proc Natl Acad Sci U S A*, 2001. **98**(22): p. 12742-7.
136. Jeffrey, P. and S. Summerfield, *Assessment of the blood-brain barrier in CNS drug discovery*. *Neurobiol Dis*, 2009.
137. Kesavapany, S., et al., *p35/cyclin-dependent kinase 5 phosphorylation of ras guanine nucleotide releasing factor 2 (RasGRF2) mediates Rac-dependent Extracellular Signal-regulated kinase 1/2 activity, altering RasGRF2 and microtubule-associated protein 1b distribution in neurons*. *J Neurosci*, 2004. **24**(18): p. 4421-31.

138. Whittaker, S.R., et al., *The Cyclin-dependent kinase inhibitor CYC202 (R-roscovitine) inhibits retinoblastoma protein phosphorylation, causes loss of Cyclin D1, and activates the mitogen-activated protein kinase pathway.* Cancer Res, 2004. **64**(1): p. 262-72.
139. Ohdo, S., *Chronopharmacology focused on biological clock.* Drug Metab Pharmacokinet, 2007. **22**(1): p. 3-14.
140. Daujat, M., et al., *Induction, regulation and messenger half-life of cytochromes P450 IA1, IA2 and IIIA6 in primary cultures of rabbit hepatocytes. CYP IA1, IA2 and 3A6 chromosome location in the rabbit and evidence that post-transcriptional control of gene IA2 does not involve mRNA stabilization.* Eur J Biochem, 1991. **200**(2): p. 501-10.
141. Pippin, J.W., et al., *Direct in vivo inhibition of the nuclear cell cycle cascade in experimental mesangial proliferative glomerulonephritis with Roscovitine, a novel cyclin-dependent kinase antagonist.* J Clin Invest, 1997. **100**(10): p. 2512-20.
142. Levi, F., et al., *Cross-talks between circadian timing system and cell division cycle determine cancer biology and therapeutics.* Cold Spring Harb Symp Quant Biol, 2007. **72**: p. 465-75.
143. Popowycz, F., et al., *Pyrazolo[1,5-a]-1,3,5-triazine as a purine bioisostere: access to potent cyclin-dependent kinase inhibitor (R)-roscovitine analogue.* J Med Chem, 2009. **52**(3): p. 655-63.
144. Sugatani, J., et al., *Induction of UGT1A1 and CYP2B6 by an antimetogenic factor in HepG2 cells is mediated through suppression of cyclin-dependent kinase 2 activity: Cell-cycle dependent expression.* Drug Metab Dispos, 2009.
145. Sadeque, A.J., et al., *Increased drug delivery to the brain by P-glycoprotein inhibition.* Clin Pharmacol Ther, 2000. **68**(3): p. 231-7.
146. Knockaert, M. and L. Meijer, *Identifying in vivo targets of cyclin-dependent kinase inhibitors by affinity chromatography.* Biochem Pharmacol, 2002. **64**(5-6): p. 819-25.